Geothermal implications of the Mourne Mountains:

constraints from magnetotelluric modelling

2010-2011

C.M. Yeomans

866475

School of Geography, Earth & Environmental Sciences,
University of Birmingham

Word count: 18,151 words

Abstract

The Mourne Granite Complex has been known as a potential geothermal energy target since 1981. Recent work since 2004 has lead to a great push for geothermal exploration in Northern Ireland (and Eire) with particular focus on the Mourne Mountains as a potential EGS target. The purpose of this study is to explore the Mourne Granite Complex in terms of its geothermal energy potential. A geophysical magnetotelluric survey collecting audiomagnetotelluric and magnetotelluric data and subsequent 2D inversion modelling of three profiles has tried to identify the shape, depth extent and volume of the subsurface granite. To understand the subsurface distribution of the granite it is important to consider the emplacement mechanism. The Mourne Granite Complex is classically thought of as the archetype for the cauldron subsidence model, however, work in the 1980s and more recently in 2007 has undermined this and suggested laccolithic emplacement. With this in mind, the survey set out to identify laccolithic structures extending from south to north towards the Mourne Granite Complex. 2D modelling has lead to three key potential targets for geothermal energy exploration which lie in both of the magmatic centres and to the south at depth. Interpretations have identified features of both laccolithic and cauldron subsidence, suggesting the emplacement mechanism may be a hybrid of the two previously proposed models. Heat flow (73.32 mW m^{-2}), heat production (mean 6.44 µW m^{-3} ±1.38) and extrapolated temperature calculations to depths of 2500 m (62.08 °C) and 5000 m (114.76 °C) have revealed promising values for geothermal energy potential in the Mourne region.

Table of Contents

1. Introduction

1.1. Project aims

This project aims to assess the geothermal energy potential of the Mourne Mountain Complex of Northern Ireland. To ascertain the geothermal energy potential, geothermal targets must be identified by the numerical inversion modelling of geophysical data. This will attempt to determine the subsurface granite in terms of its shape, depth extent and volume. Numerical inversion modelling will be based on magnetotelluric data collected from three profiles across the Mourne area. The geothermal energy potential of the Mourne Mountains can also be quantified and assessed through heat flow, heat production and temperature calculations. These calculations will be based on pre-existing data from the Northern Irish TELLUS project (see van Dam 2007), Geothermal Energy Resource Map of Ireland (see Goodman *et al.* 2004), Deep Geothermal Exploration Drilling Programme Completion Report (see Kelly 2010), as well as petrophysical data (see Antriasian 2010) and unpublished x-ray fluorescence data (see Reay 2011). It is through the combination of geophysics to define the shape, depth extent and volume as well heat flow, heat production and temperature calculations that we hope to identify potential geothermal targets in the Mourne area.

N.B. Herein, the processing, analysis and modelling of the three magnetotelluric profiles (named EMC, WMC and SLA) are discussed without reference. It should be noted that processing, analysis and modelling of EMC was undertaken by Laura Ayres. Processing, analysis and modelling of WMC and processing and modelling of SLA was undertaken by myself. Analysis of SLA was undertaken by Dr Mark Muller (DIAS).

1.2. Background

The Mourne Mountains are located in County Down, southeast Northern Ireland (Fig. 1.1.). The highest point in the region is Slieve Donard at 853 m with seventeen other peaks in the Mourne area reaching over 500 m.

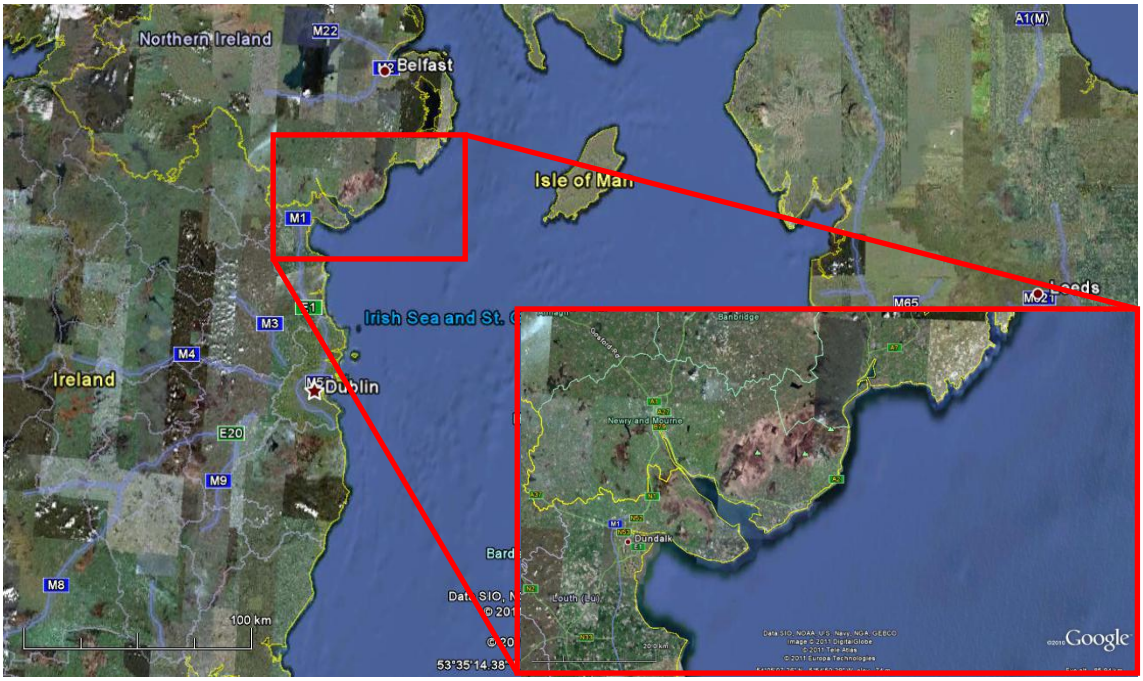

Figure 1.1 Location map for the Mourne Mountains, Northern Ireland (Google Earth 2011)

The Mourne Mountains are predominantly made up of granite with a component of composite-felsic dykes. It was emplaced during the Palaeogene and forms part of the British [and Irish] Palaeogene Igneous Province (BPIP). The country rock surrounding the Mourne Mountains is of Silurian age composing of greywackes and siltstones of the Southern Uplands-Down-Longford terrane (Anderson 2004). Granite rocks in the area are highly resistive with resistivities in the range of 10,000-30,000 Ω.m (Kelly 2010) which is in contrast to the relatively conductive greywackes and siltstones which have an estimated resistivity of 50-500 Ω.m (see Fig.1.15; from Miensopust 2010 adapted from Palacky 1987 and Martí 2006). It is this difference in resistivity between the granite and country rocks that make the magnetotelluric technique ideal for investigating the subsurface distribution of the granite in this area.

1.2.1. Geology

Silurian greywackes and siltstones are the dominant rock type in the Mourne region and form the country rock to the Mourne Mountain Complex. The Silurian greywackes and siltstones form part of the Southern Uplands-Down Longford terrane which is bounded by the Southern Uplands fault to the north and the Navan fault (representing the Iapetus suture) to the south (Anderson *et al*. 2004). The Southern Uplands-Down-Longford terrane is interpreted as the accretionary prism of the Iapetus Ocean in a fore-arc setting relating to subduction during the Ordovician and Silurian (Anderson *et al*. 2004). It is this very accretionary prism which stretches from Scotland, through Northern Ireland

and into Ireland that threw up the 'Southern Upland Paradox'. The paradox was formed through an ambiguous younging direction based on biostratigraphy (younging to the SE) which did not correlate with bed dip to the NW. This was solved by the realisation of strike-parallel underthrusting during subduction creating a structural younging toward the NW but a stratigraphic younging toward the SE against the dip of the beds (Anderson *et al.* 2004). In the Late Silurian, oblique collision of the Laurentian and Avalonian land masses produced the Caledonide Mountains and mildly deformed the Southern Uplands-Down-Longford terrane (Anderson 2004; Anderson *et al*. 2004).

The Mourne Mountain Complex is intruded into the Hawick Group of the Southern Uplands-Down-Longford terrane which lies within the 'Central Belt'. The 'Central Belt' corresponds to graptolite divisions and is attributed to the Early Silurian (Lapworth 1878). The Hawick comprises of greywackes, siltstones and mudstones rich in carbonate (Anderson 2004). Bedding trends ENE-WSW generally steeply dipping toward the NNW (Anderson 2004). It is interpreted as a well-bedded, proximal-distal turbidite sequence which largely contains siltstones and mudstones in the Mourne area (Anderson 2004). Deformation within the Hawick group has been split into three structural facies based on folding and these reflect the rheology of the sediments within each facies. Folding is associated with subduction and stripping of sediment into the accretionary prism (Anderson 2004). There are two later phases of ductile deformation which are quite weak in this area (Anderson 2004). Caledonian strike-slip faulting (mainly sinistral) is common in the area but with only small amounts of displacement and reflects the oblique collision of Laurentia and Avalonia (Anderson 2004; Anderson *et al*. 2004). Metamorphism is of low grade in the Hawick Group and in the Mourne area is mainly of zeolite facies (Anderson 2004). Studies of contemporaneous sediments in Scotland indicate a maximum burial depth of 12 km due to underthrusting based on illite crystallinity (Merriman & Roberts 2001).

The Mourne Mountain Complex is a Palaeogene intrusive suite of felsic rocks (forming part of the BPIP). They were emplaced at a high level in the crust at ~56 Ma, however, there is no evidence of extrusive magmatism in the area (Gibson *et al*. 1988; Gamble *et al*. 1999; Cooper & Johnston 2004). The intrusive rocks of the BPIP are concentrated in Country Down and County Armagh (and County Louth, Eire), these rocks comprise the Mourne Mountain Complex, Carlingford Complex and Slieve Guillion Complex (Cooper & Johnston 2004). These suites consist of granites, felsites and granophyres but also large volumes of mafic rocks such as the basalt, dolerite and gabbro which make up

the Carlingford and Slieve Guillion Complexes (Cooper & Johnston 2004). It is thought that Palaeogene magmatism is related to the Iceland Plume which was located below the east coast of Greenland at the time (Cooper 2004). The area affected by the plume had a diameter up to 2000 km and it impinged on the base of the lithosphere along the western coast of the British Isles to produce large amounts of both felsic and mafic magma (Cooper 2004). Magmatism is particularly prevalent in Northern Ireland due to a failed Palaeocene rift relating to the opening of the Atlantic Ocean, this allowed for extension, dilation and uplift resulting in favourable conditions for high-level magma emplacement where extrusion is common (e.g. County Antrim) (Cooper 2004).

The Mourne Mountain Complex consists of five granites dubbed G1-G5. Originally these were G1-G4 after Richey (1927) and were later revised by Hood (1981) and Gibson (1984). G1-G3 occur in the eastern magmatic centre with G4 and G5 observed in the western magmatic centre. These 'G' facies are further subdivided by textural and compositional variations. Gravity data by Cook & Murphy (1952) suggested more dense, mafic rocks underlay the granite plutons. The different facies attributed to the granites in the Mourne area are thought to relate to pulse events in the region which become progressively more felsic and may represent the fractional crystallisation of a crustally contaminated basalt melt (Hood 1981; Gibson *et al*. 1988; Meighan *et al*. 1992; Cooper & Johnston 2004). Textural variations do not show such a temporal relationship and can be coarser or finer than the previous pulse.

Small outcrops of country rock can be found on various peaks in the Mourne Mountains with a sliver trapped within G2 on the easternmost edge of the granite complex near Slievenagarragh (Cooper & Johnston 2004). Metamorphism due to the granite is localised with only a small metamorphic aureole (Stevenson 2011, *Pers. Comm.*) forming diopside- and biotite-hornfels in the Silurian siltstones and mudstones (Cooper & Johnston 2004).

1.2.2. Emplacement mechanisms of the Mourne Granite Complex

Understanding the emplacement mechanism for the Mourne granites is imperative for predicting the subsurface distribution of granite at depth and thus assessing the geothermal potential of the area.

The Mourne Mountains was first studied in detail by Richey (1927) through geological mapping (Fig. 1.2.). Based on his work that primarily focussed on the eastern magmatic

centre, Richey proposed a cauldron subsidence model (Fig.1.3.) that made use of a steep feeder wall in the east with a roof formed by G1 which was the outermost granite facies. Later pulses would then move up the eastern wall conduit and force a subsiding block downwards.

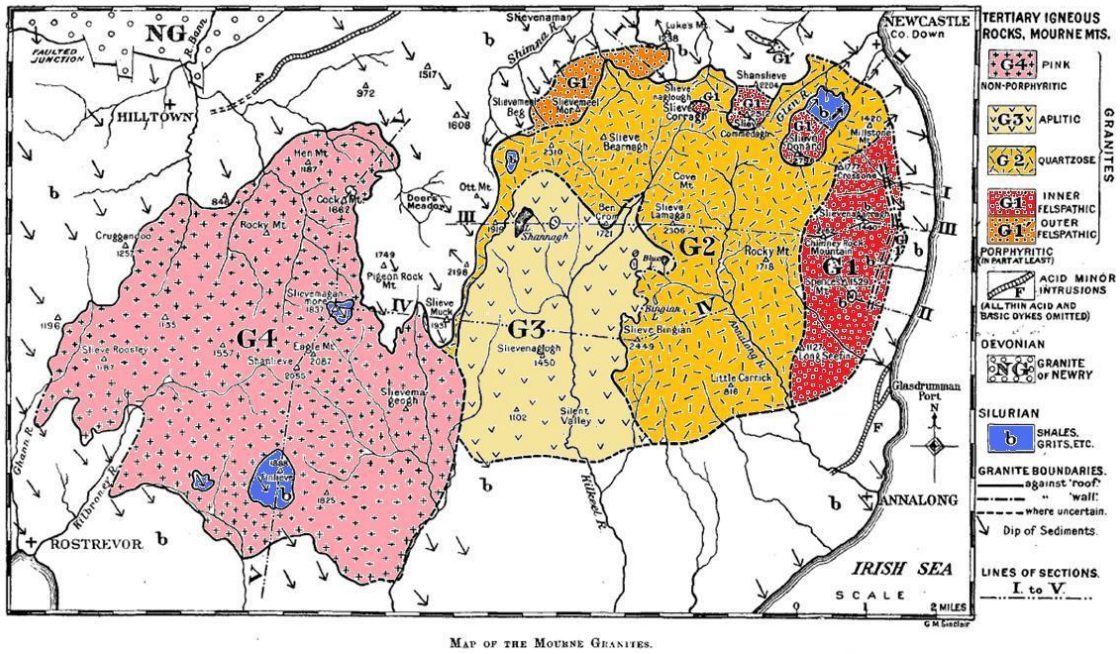

Map of the Mourne Granites.

Figure 2 Geological map of the Mourne Mountains showing the different granite facies as mapped by Richey (1927) (adapted from Richie 1927)

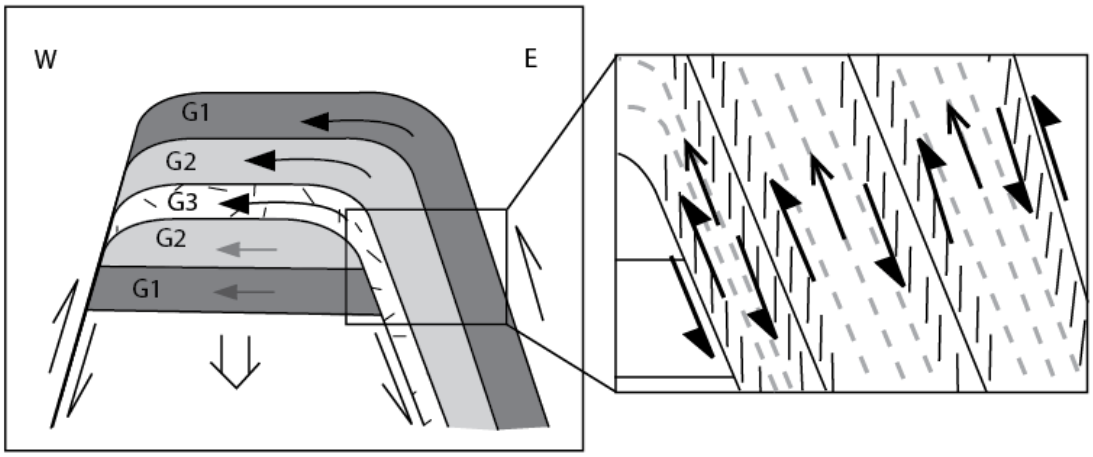

Figure 3 Details of Richey's cauldron subsidence model (from Stevenson *et al.* 2007)

This model also requires a shear zone in the western flank of the intrusion which may be complicated by the intrusion of the western magmatic centre. These features described by Richey are predominantly shown in E-W cross section. The northern and southern boundaries are inferred to be steep.

Although Richey's model became generally accepted and the Mourne Mountains became a one of the most well known examples for cauldron subsidence there was some opposition. Rohleder (1932) proposed a discordant laccolithic model. Walker (1975) suggested intrusion of magma laterally westwards into a favourable zone of localised lower pressure caused by the subsidence of nearby mafic intrusive rocks. This was described by Walker as a 'curved flange' model. Neither of these models gained wide acceptance as they were not supported by field evidence (see Stevenson *et al*. 2007).

Revisions through geological mapping by Hood (1981) and Gibson (1984) resulted in the validity of the cauldron subsidence model and Walker's curved flange model being called into question. Revisions meant that the large majority of what was classed as 'G1' was reattributed to 'G2 outer' leaving G1 remaining on the peaks of Slieve Donard and Slieve Commedagh. Despite this, cauldron subsidence in the eastern magmatic centre was the most favoured emplacement mechanism and Hood (1981) simply revised Richey's model despite acknowledging components of laccolithic emplacement (Fig.1.4.).

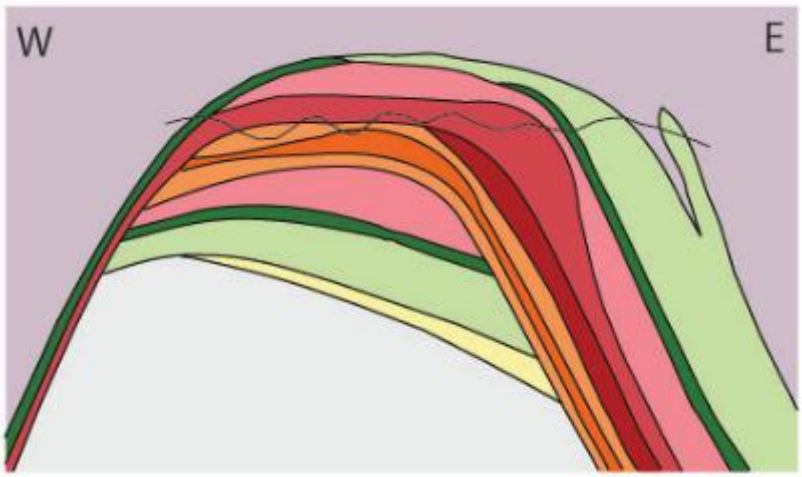

Figure 1.4 Cauldron subsidence model as proposed by Hood 1981. A modified version of Richey's model (from Ayres *et al*. 2011; adapted from Hood 1981)

Evidence of field relationships from Hood (1981) and later Meighan *et al*. (1984) essentially undermined the cauldron subsidence model but until recently remained the over-riding theory due to lack of an alternative hypothesis.

Recent work by Stevenson *et al*. (2007) using anisotropy of magnetic susceptibility (AMS) has lead to the development of laccolithic emplacement model for the eastern magmatic centre. This is accompanied by work on the western magmatic centre

(Stevenson & Bennett 2011) which describes a similar flow model with flow parallel to that of the eastern magmatic centre (Fig.1.5.).

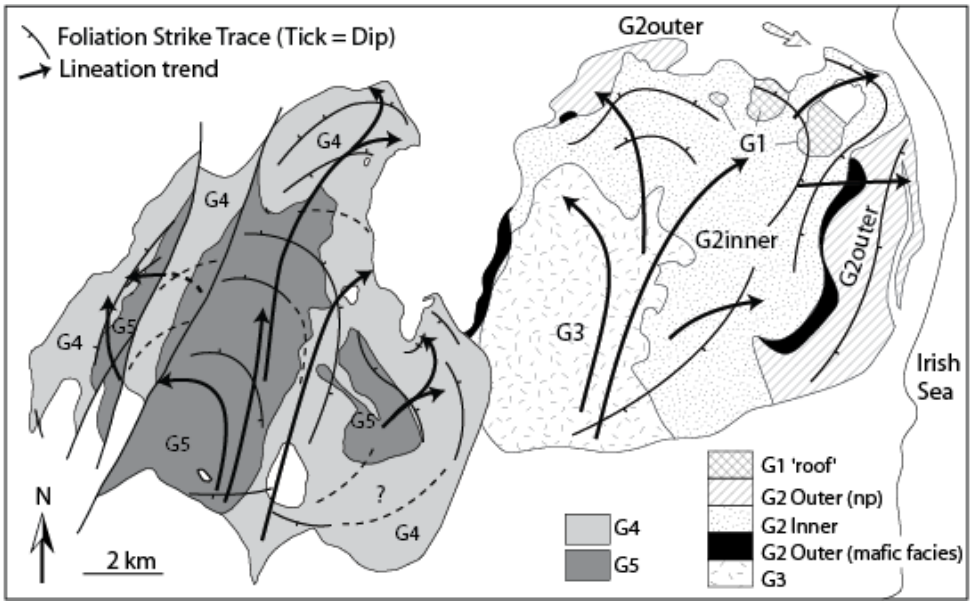

Figure 1.5 AMS flow directions for the eastern and western magmatic centres (from Stevenson & Bennett 2011)

This laccolithic model with flow from the SSW toward the NNE is supported by a gravity high to the SW of the Mourne Mountains beneath Carlingford Lough (see Cook & Murphy 1952; Wright *et al*. 1971; Reay 2004). This gravity high is interpreted as a potential mafic feeder zone for the Mourne Mountain Complex (Stevenson *et al*. 2007) and extends laterally from Slieve Guillion to south of the Mourne Mountains (Reay 2004). If the gravity high does relate to a mafic feeder zone this may provide a genetic link between a crustally contaminated basaltic melt (Hood 1981; Gibson *et al*. 1988; Meighan *et al*. 1992; Cooper & Johnston 2004). Although a mafic feeder zone has been inferred from gravity data, actual modelling of the gravity signature to define the density, shape and depth extent of the causative body has not been done. Gravity modelling must be done before a mafic source region can be attributed to the gravity anomaly.

Despite inferences of flow from south to north, ambiguity in the AMS fabric and its use as a proxy for flow direction results in the possibility that magma flow was from NNE to SSW. Such a scenario would lend weight to a curved flange model (*sensu* Walker 1975; Stevenson *et al*. 2007), however, this has implications for drawdown of a buoyant felsic magma and may not be plausible. Also, no source region is apparent to the north and thus may mean viscous, felsic magma from the south would be travelling long distances below the region to then flow back toward the source.

The laccolithic model proposed by Stevenson *et al*. (2007) and reinforced by Stevenson & Bennett (2011) is supported by field evidence of intermediate to low-angle dipping contacts within the eastern magmatic centre (Hood 1981; Stevenson *et al*. 2007). Field relationships also contradict findings by Richey showing that the G2-G3 boundary is gently dipping, not steep, as Richey's steep walled model implies (Stevenson *et al*. 2007). Minor shear zones have been identified with localised dark deformation bands relating to emplacement and cooling of magma and subsequent intrusion of later magma (Stevenson *et al*. 2007). Stevenson *et al*. (2007) propose that gently dipping fabrics with evidence for a domed pluton suggest inflation of a sheet-like granite body or laccolith (Fig.1.6.). Steep contacts in the east are explained by sub-solidus deformation due to inflation of an underlying sheet (Stevenson *et al*. 2007)

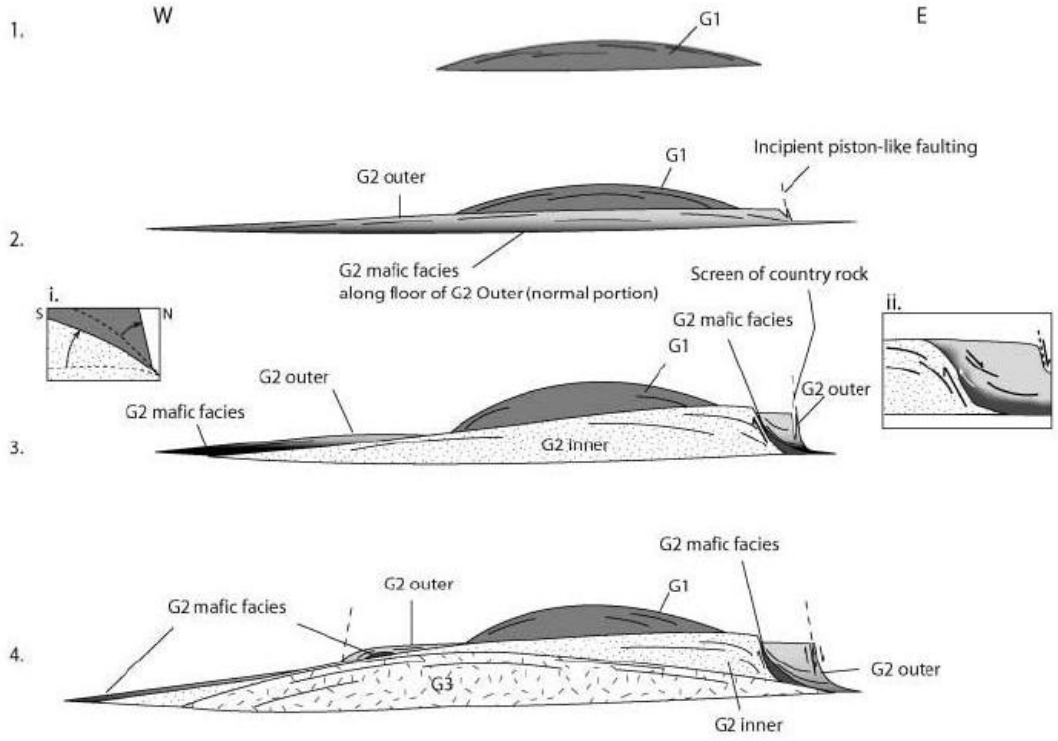

Figure 1.6 Laccolithic emplacement model for the eastern magmatic centre (from Stevenson *et al.* 2007). The model shows the emplacement of each facies, however, does not determine the depth extend of the laccolith

The laccolith model and cauldron subsidence model vary greatly in their emplacement mechanism and have substantially different implications for the subsurface distribution of granite at depth. Cauldron subsidence would infer a stock-like body approximate to an upright cylinder of granite. This is in contrast to a laccolithic emplacement which would infer a layered, laterally extensive granite body at depth where thicknesses may vary.

The thickness of the granite in the discussed models is difficult to determine. Richey (1927) makes little mention of the depth extent of his stock-like granite body with subsiding block. His original model has an approximate outcrop length at the surface (running east-west) of 7 miles (~11.5 km), if no vertical exaggeration is assumed for the model, a depth extent of 5km can be inferred to the top of the subsided country rock block and >10 km in the eastern wall conduit (Fig.1.7.).

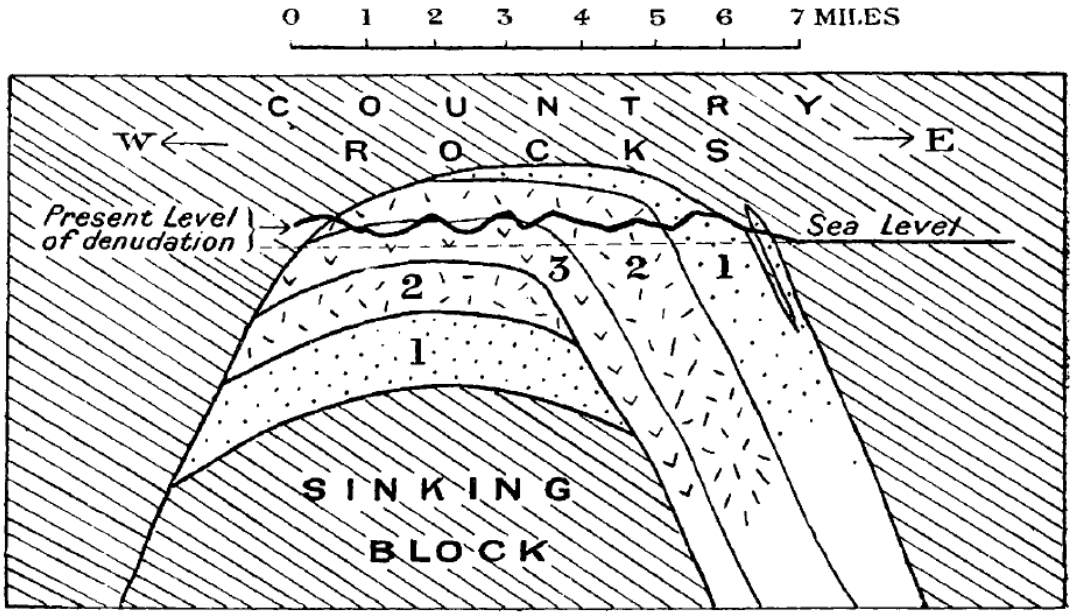

Figure 1.7 Original cross-section from Richey (1927) with a horizontal scale inferred. Assumption is that no vertical exaggeration is applied.

Models by Stevenson *et al*. (2007) and Stevenson & Bennett (2011) do not discuss a depth extent to their laccolithic models. Laccolithic granites can range from as little as 1 km thick for a 'single sheet' laccolith (Aranguren *et al*. 2003) up to >5 km for a multilayered or 'christmas tree' laccolith (Westerman *et al*. 2004).

It is more than reasonable to say that the shape and depth extent of the Mourne Granite Complex is poorly understood. Preceding our work, the shape, depth extent and consequently the volume of the body has not been given the consideration it needs for determining geothermal energy potential in the Mourne area.

1.2.3. Geothermal potential of the Mourne Mountains

Irish geothermal exploration was first begun by Wheildon of Imperial College, London (summarised in Čermák & Rybach 1979). The Mourne Mountains were first identified as a geothermal target by Monnet (1981) and further explored through work by Brock &

Barton (1984) and Brock (1989). Brock (1989) presents a suite of data from several projects across Northern Ireland and Ireland (Fig.1.8.).

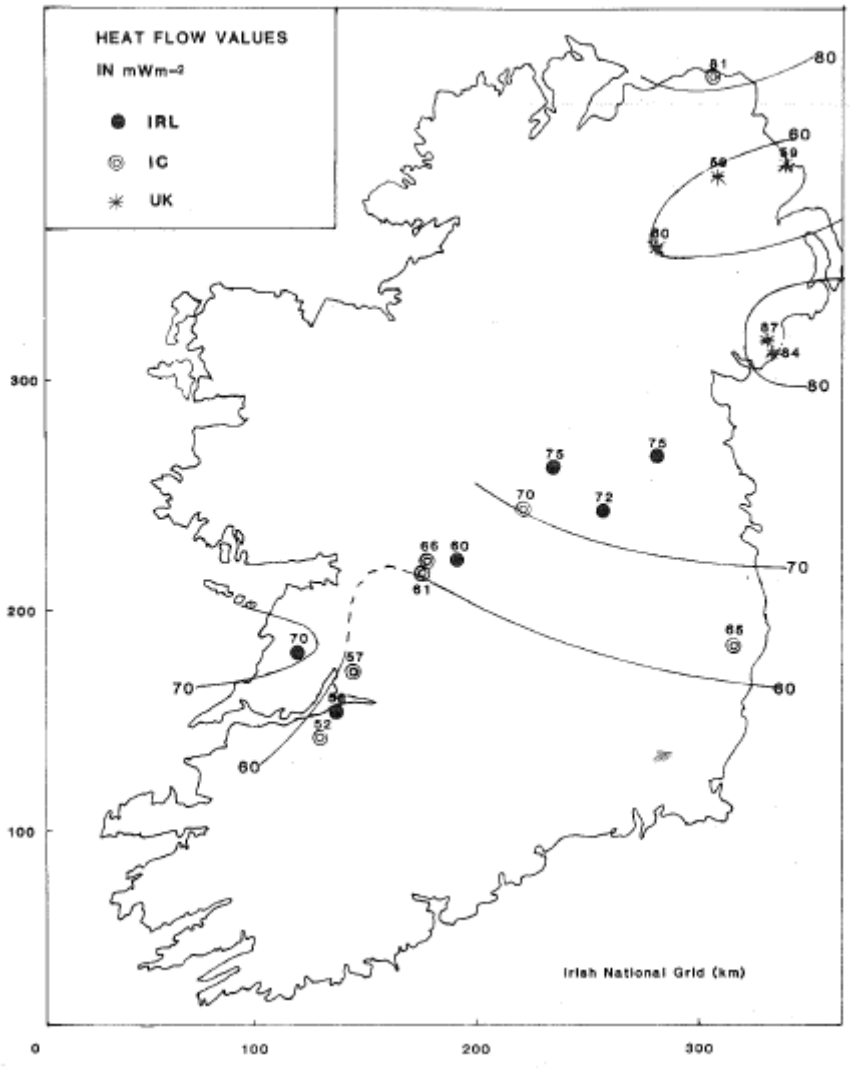

Figure 1.8 Heat flow measurements from Brock (1989) showing two data points omitted by Goodman *et al.* (2004)

Temperature and heat flow values at the time was largely constrained within the bounds of the Southern Uplands fault and Iapetus Suture. This is due to many boreholes being drilled to exploit mineralogical resources in Carboniferous overburden (Brock 1989) and means significant gaps exist in the data. The majority of the boreholes are deep and it is deemed unnecessary to account for climatic change due to the depth, however, two boreholes are <150 m and have had climatic correction applied (described in detail by Wheildon *et al*. 1985). It is these two shallow boreholes which bare the most significance to this project found in the Annalong Valley and Seefin Quarry (near Glasdrumman) which have heat flow values of 87 mW m^{-2} and 84 mW m^{-2} respectively. Values presented by Brock (1989) range from 57 mW m^{-2} to 87 mW m^{-2}, averaging

71 mW m^{-2}. The values for the Mourne area and other values are much higher than the expected values for their tectonic age and also the UK average for sedimentary crust, of which are both, coincidentally, 55 mW m^{-2} (Rollin 1987).

More recent work by Goodman *et al*. (2004) has modelled surface heat flow (Fig.1.9.) and temperature at 2500 m depth (Fig.1.10.) for Northern Ireland and Ireland.

Surface heat flow variation was measured and modelled revealing a general trend of increasing surface heat flow toward the north from ~50 mW m^{-2} in County Cork and County Clare up to ~80 mW m^{-2} in County Donegal and Northern Ireland (Goodman *et al*. 2004). This apparent regional trend is likely to be governed by the Late Cretaceous – Palaeocene extension in Northern Ireland relating to early stage rifting of the Atlantic Ocean (*c.f.* Cooper 2004). Controls on this trend can be suggested such as crustal thickness, lithospheric thickness, average crustal heat production or any combination of these, however, this has not been modelled and is currently unknown. The modelled map of surface heat flow crucially omits the two readings in County Down included by Brock (1989). This is likely due to the shallow borehole depth at both sites and reliability of the data and climatic correction factor. If we assume these data points are in principle reliable, heat flow of 84 and 87 mW m^{-2} would have a profound effect on the modelled data, particularly in southeast Northern Ireland.

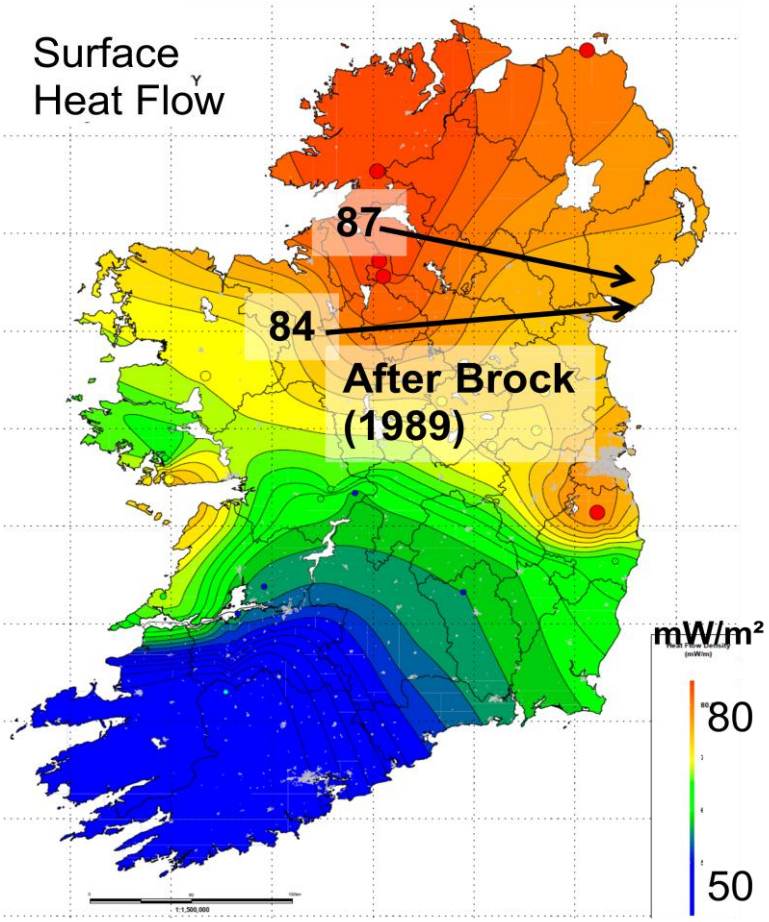

Figure 1.9 Surface heat flow modelling from Goodman *et al.* (2004) showing values of ~70 mW m-2 with values from Brock (1989) illustrated.

The surface heat flow is a function of the thermal conductivity of the rocks the geothermal gradient:

(1) $$Q = k\frac{\Delta T}{\Delta z}$$

Where Q = heat flow, k = thermal conductivity, ΔT = change in temperature and Δz = change in depth.

Many of the data points only sample Carboniferous strata which are characterised by limestones with low thermal conductivities this would infer that the geothermal gradient is exaggerated and thus, projected temperatures at depth will be overestimated which will then overestimate future modelling values (Goodman *et al*. 2004). By omitting the measurements by Brock (1989) the projected heat flow for the Mourne area may well be underestimated.

The modelled temperature at 2500 m depth includes 49 data points to constrain the model, however, only two of these are measured borehole temperatures at 2500 m

depth, the remaining are extrapolations based on boreholes >500 m depth in which the bottom-hole temperature is used with a well constrained geothermal gradient to estimate temperature at depth.

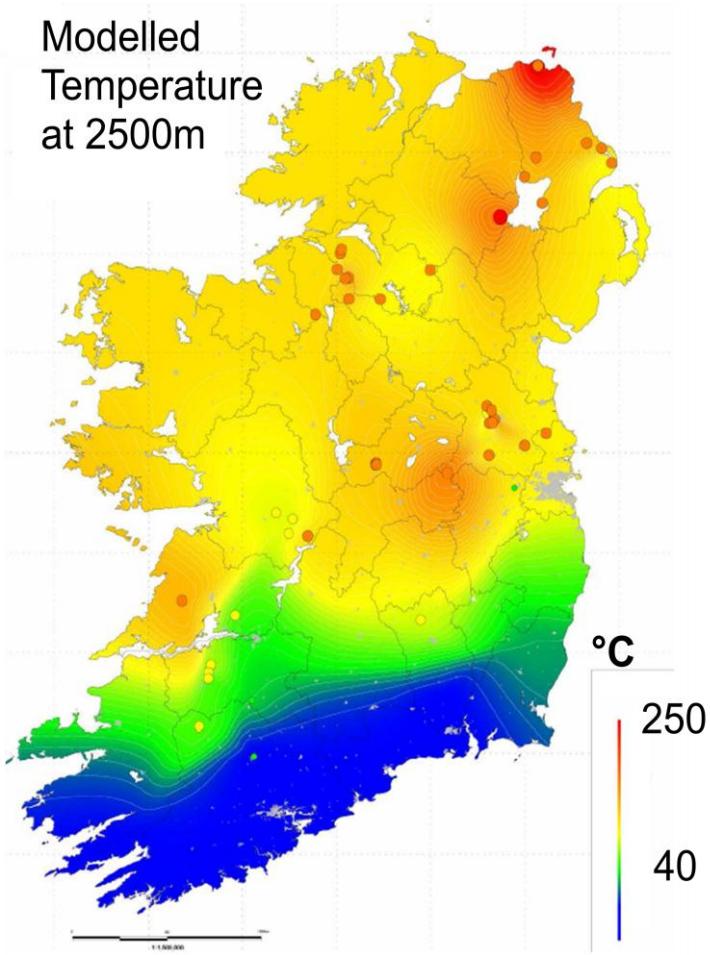

Figure 1.10 Temperature modelling from Goodman et al. (2004) showing values of ~60 °C for the Mourne area.

The modelled temperature at depth has not had an elevation correction applied and may therefore give a slightly distorted model, however, discrepancies are of a maximum 4.75 °C (Goodman *et al*. 2004). Despite the increased number of data points used by Goodman *et al*. (2004) there is still comparatively poor coverage across Ireland as a whole with significant omission of older metamorphic and igneous complexes.

Temperature at depth is extrapolated from borehole measurements using average temperature gradient and bottom-hole temperatures.

Heat production is an important factor to consider on its own too. Heat production is the natural amount of radiogenic heat produced by a rock measured in µW m^{-3}. Contributions to heat production largely come from radiogenic isotopes of potassium

(K), thorium (Th) and uranium (U). Measurements of radiogenic isotope concentrations in Northern Ireland were collected as part of the TELLUS Project (Fig.1.11.; data courtesy of GSNI). This is presented as ternary data on a map of Northern Ireland.

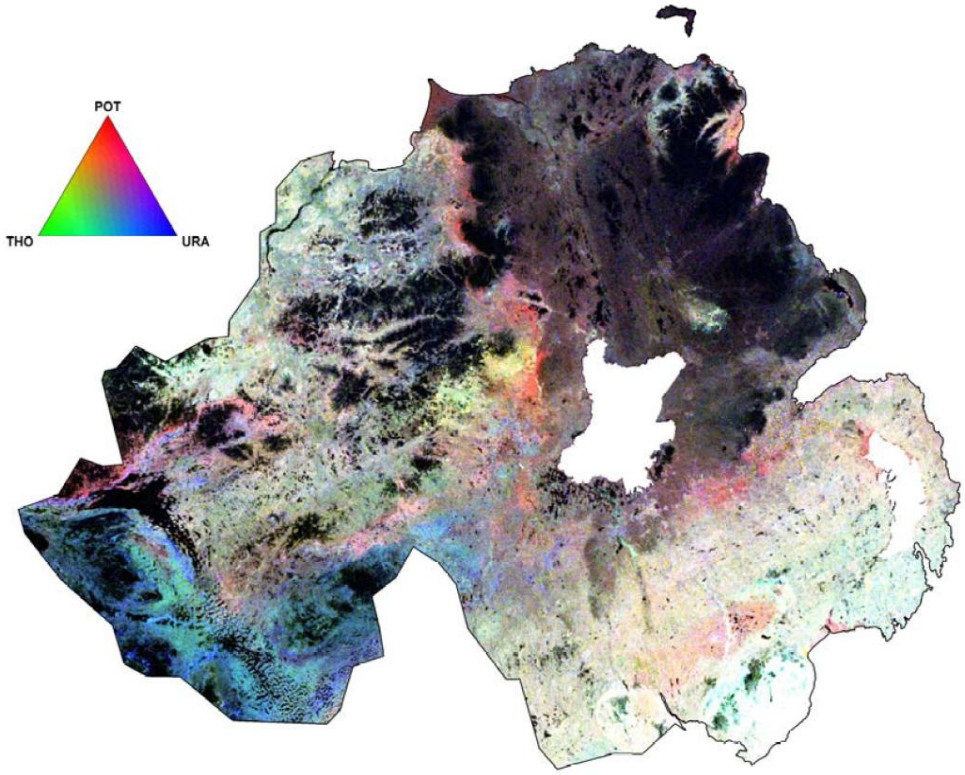

Figure 1.11 TELLUS aerial radioelement concentrations for Northern Ireland (courtesy of GSNI) showing a white hotspot over the Mourne area indicating high concentrations of all three elements (U, Th, K).

The ternary data shows that a white 'hotspot' (representing high concentrations of all three radiogenic elements) can be seen over the Mourne Mountains. The data also shows surprising detail relating to the Southern Uplands-Down-Longford terrane with a fabric oriented ENE-WNW and a relative reduction in Th and U towards the northern part of the terrane – this would be due to the more coarse, greywackes dominating over siltstones and mudstones of the Early Silurian (Anderson 2004). The hotspot of radiogenic isotopes in the Mourne area is of direct consequence of the composition of the granite (Stevenson 2011, *Pers. Comm.*) and this has fundamental implications for heat production. TELLUS radiometric data were modelled for heat production by van Dam (2007). Heat production was calculated by gridding TELLUS data for each radiogenic element and computing the radiogenic heat production for each grid square using the following equation:

(2) $$A = 0.337(0.74eUppm + 0.199eThppm + 0.26K\%)$$

Where A = radiogenic heat production, eUppm = estimated Uranium concentration in parts per million, eThppm = estimated Thorium concentration in parts per million, K% = potassium concentration as a percentage (*from* van Dam 2007; *after* Carmichael 1989).

The first heat production equation was originally proposed by Rybach (1976) and updated by Rybach (1988) and then Carmichael (1989) with more accurate constants (*c.f.* van Dam 2007). The use of 'e' relates to estimated concentration of U and Th in part per million (ppm). K is measured as a percentage.

Results of the calculation by van Dam (2007) for the Mourne Mountains are displayed below (Fig.1.12.):

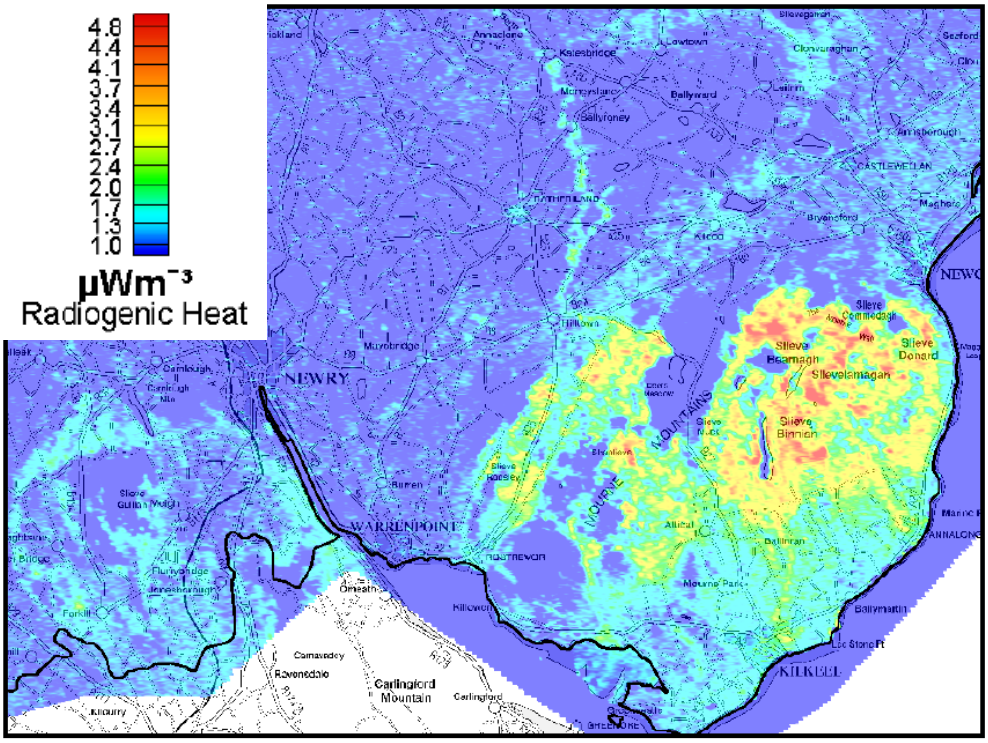

Figure 1.12 Gridded and calculated radiogenic heat production from van Dam (2007) showing highest heat production in the eastern magmatic centre.

The data show a considerable increase in heat production in the granitic areas of the map with Silurian country rock being of very low heat production despite having apparent high radiogenic isotope concentrations (see Fig.; TELLUS aerial radiometric data). There is also a noticeable difference in the calculated heat production between the eastern and the western magmatic centres (Fig.1.13.). Isotope data from McCormick *et al*. (1993) and Meighan *et al*. (1988) highlight variations between the different granite

facies. Isotope data indicates that G1 and G5 are both less evolved than G2, G3 and G4. A less evolved magma is likely to have a lower radiogenic element concentration and thus a lower heat production.

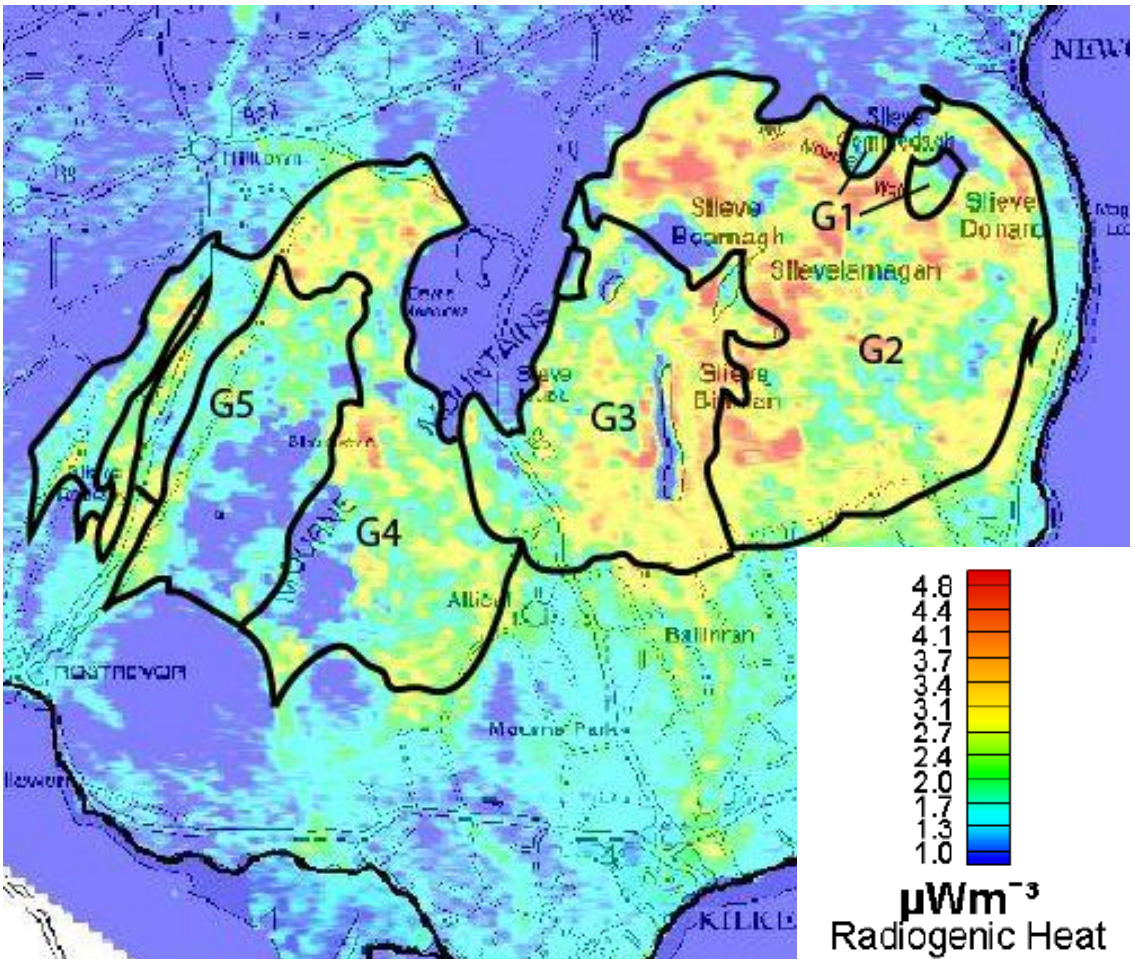

Figure 1.13 Radiogenic heat production with overly of the different granite facies to outline potential correlations between facies and heat production (adapted from van Dam 2007)

This may be a key point to consider in terms of geothermal energy potential due to the significant decrease in heat production associated with the western magmatic centre. Low heat producing granite rocks are much less desirable.

It is worth noting that despite some key inferences from the radiogenic heat production map by van Dam (2007), it is based on surficial data with a penetration of a few centimetres (Desissa Ture, 2011, *Pers. Comm.*). This may not be representative of heat production at depth and is certainly not a proxy for subsurface granite distribution. This data was also collected from an aerial survey and is not directly measured from surface sampling or hand specimen geochemical analysis.

1.2.4. Principles of an Enhanced Geothermal System

The Mourne Mountains, being an inactive igneous system with no hydrothermal circulation, if determined to be geothermally prospective, would need to be exploited as an Enhanced Geothermal System (EGS), also known as an Engineered Geothermal System (EGS) or Hot Dry Rock (HDR) geothermal system. Herein, EGS will be used in terms of an Enhanced Geothermal System.

The principle of an EGS as a geothermal reservoir is to use hot rocks with a high heat producing capacity to heat up a fluid (usually water). This is done by using one or more drill holes to inject fluids into an artificial reservoir created through 'fracking' and forcing this to return to the surface through another drill hole under the pressure of the injection fluid (Fig.1.14.).

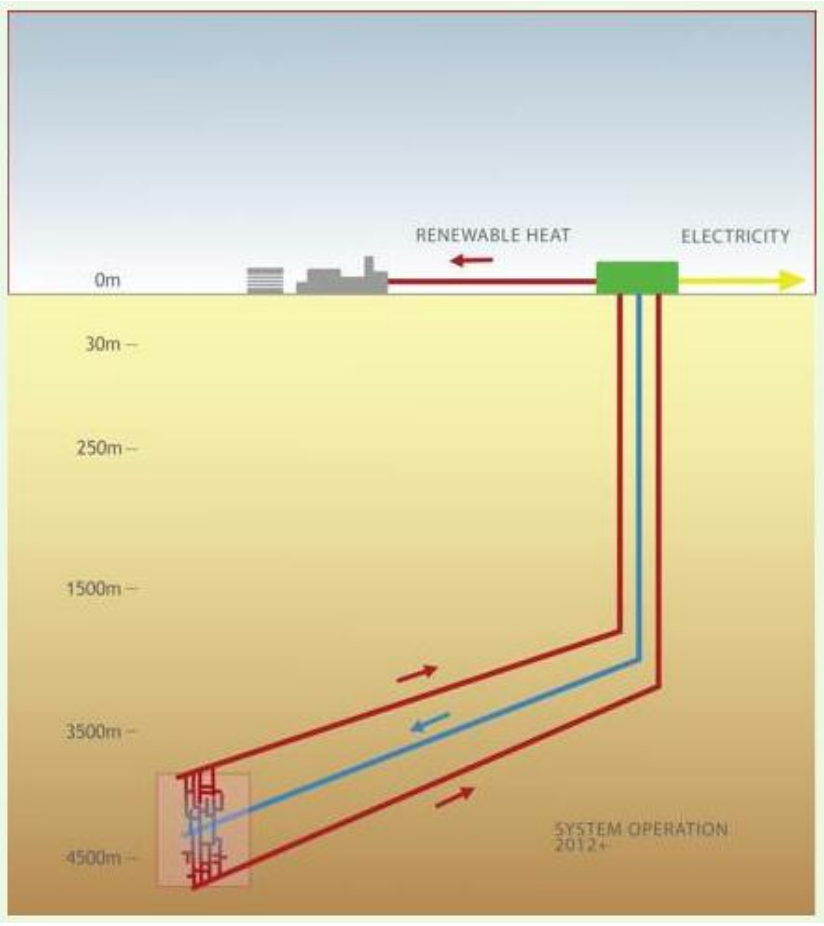

Figure 1.14 Example of an EGS system using three drill holes connected by a fracture network (Geothermal Engineering Ltd 2011)

Once returned to the surface the hot fluid can be used to produce electricity either directly if it returns as steam, through a flash system to turn the hot water to steam, or through a binary system where the hot fluid is used in a flash system to vaporise another

fluid with a lower boiling point. Alternatively low enthalpy geothermal reservoirs can be exploited in similar ways for space heating.

For an ideal EGS target, the following criteria must be satisfied:

- An elevated local/regional temperature gradient.
- A high radiogenic heat production.
- A depth extent to 4-5 km.
- A large volume.

Mineral fabrics and the orientation of joints as well as the overall stress field acting upon the Mourne Granite Complex are also important characteristics to consider when assessing the geothermal viability of the area. When creating an artificial reservoir the overriding stress field must be considered as the injection of fluid may result in shearing and failure in unfavourable orientations.

It is evident that particularly the eastern magmatic centre of the Mourne Mountains would appear to have a high radiogenic heat production (see van Dam 2007). A reasonable high temperature gradient can be inferred for the whole of Northern Ireland from examining the surface heat flow modelling (see Goodman *et al*. 2004). A depth extent to 4-5 km and a large volume are the main investigative aims of the magnetotelluric survey.

1.3. Magnetotelluric Theory

Material in this chapter has largely been drawn from Simpson & Bahr (2005) and Miensopust (2010). A more detailed practical summary is provided in Miensopust (2010) to which the reader is referred.

The magnetotelluric (MT) method was first outlined by Tikhonov (1950) and elaborated in detail by Cagniard (1953). MT is an electromagnetic geophysical technique where a natural, ambient source is used to measure geoelectrical properties of underlying rocks. Cagniard (1953) detailed full equations and implications for the magnetotelluric method and the interactions of electric currents in the earth with magnetic and electrical currents at the Earth's surface. The most controversial assumption by Cagniard (1953) is that the source field is a plane wave source and this was highlighted by Wait (1954). Work was also needed to represent the electrical and magnetic fields in a laterally conductive medium. This led to computer modelling showing that Cagniard's assumption is correct

for mid-latitudes for periods up to 10^5 s (Swift 1967; Madden & Nelson 1986). Further work was done in determining the admittance (Bostick & Smith 1962) or impedance tensor (Berdichevsky 1960; Tikhonov & Berdichevskiy 1966). The method presented by Bostick & Smith (1962) became popular as it allowed for the minimisation of diagonal components of the electrical and magnetic fields to a comparable state similar to that of Cagniard (1953).

1.3.1. Natural electromagnetic sources

Electromagnetic sources involved in MT are ambient, they are not controlled. In MT data acquisition the electromagnetic field is sourced from the ionosphere. This is the result of interactions of ionised particles in the atmosphere with the solar wind. The solar wind creates a secondary field within the ionosphere which cancels out the Earth's natural magnetic field. The point where the Earth's magnetic field ceases is known as the magnetopause. The magnetopause does not form concentrically around the Earth but is stretched outwards away from the Sun and compressed closer to the Earth on the side facing the Sun. Induction of currents can occur in the ionosphere which interact with the magnetopause and produce diurnal forces. The diurnal force is a combination of the interaction of the ionosphere, magnetopause (and thus magnetosphere) and the solar wind. This source fluctuates daily, seasonally and on an 11-year solar cycle to cause variation in signal strength (Garcia & Jones 2002). These diurnal forces can have long periodicities (>1 s) which have great penetration into the Earth.

High frequency MT data are generally known as audio-magnetotelluric (AMT) data. AMT data have a different source to the MT electromagnetic fields where AMT sources originate from meteorological effects in the form of lightning storms. Despite the apparent random and chaotic nature of a single lightning strike there is a surprisingly consistent base level when the whole Earth is considered. Lightning storms provide a strong source of high frequency (low periodicity) electromagnetism with sensitivities ranging 1 – 10,000 Hz. The electromagnetic fields produced by a lightning strike propagate through the atmosphere great distances, trapped between the Earth's surface and the ionosphere (Garcia & Jones 2002; Simpson & Bahr 2005). Garcia & Jones (2002) demonstrated that AMT data acquisition is best conducted at night due to a lower atmospheric conductivity and thus less attenuation of the electromagnetic field. In Britain, data acquisition over night, particularly in summertime, corresponds to peak hours of sunlight in low-latitude tropical regions such as the Caribbean (Hogg 2010;

Pers. Comm.). This in turn is approximate to peak lightning activity in the Caribbean and provides a good AMT source field at a time when atmospheric attenuation is at a minimum.

This distant source field is fundamental to the magnetotelluric method. It is the reason magnetotellurics varies from controlled source electromagnetic surveys as it allows the assumption of a plane wave source field (see Cagniard 1953).

1.3.2. Electromagnetic properties in rocks

The MT method measures the electrical permittivity (ε) and resistivity (ρ) of rocks as well as their magnetic permeability (μ).

Electrical Permittivity

The electrical permittivity (ε) of a rock is a measure of its ability to transmit an electric field. It also is a measure of the ability of a rock to become polarised by an applied electric field, thus reducing the total electric field within the rock (Miensopust 2010).

The electrical permittivity is an important parameter in displacement currents which are negligible for this study (see Section 1.3.3.) and will not be discussed further.

Resistivity

Electrical resistivity (ρ) (or its reciprocal, conductivity; σ) is a measure of a rocks ability to conduct electric current. It is controlled by Ohm's Law (see Section 1.3.3.) relating current density, the applied electric field and the rock conductivity. The conductivity is a tensor quantity, however, due to the assumption in the MT method that it is the bulk conductivity of a rock that is measured (thus the rock is assumed to have isotropic conductivity), conductivity can be treated as a scalar quantity (Miensopust 2010). It should be noted that inversion codes do exist that can account for anisotropic conductivities. Resistivity values for rocks are displayed below (Fig.1.15)

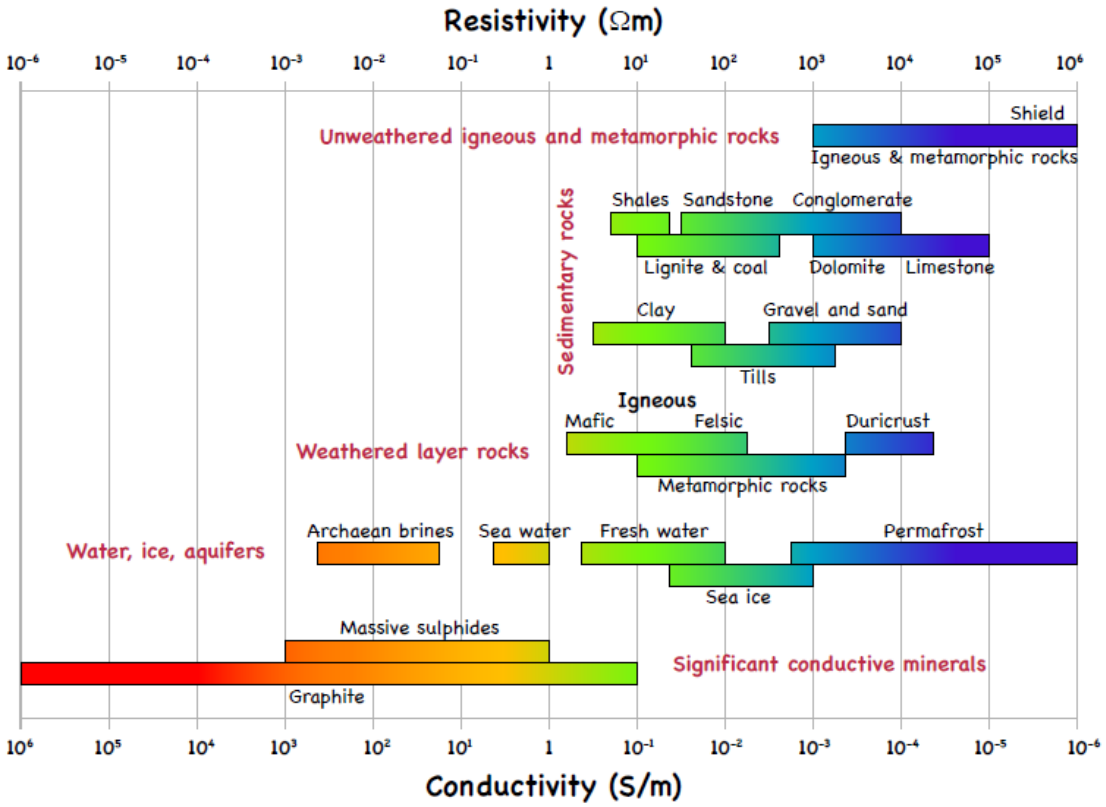

Figure 1.15 Resistivity and conductivity for various rock types (from Miensopust 2010; adapted from Palacky 1987 and Martí 2006)

Magnetic Permeability

The magnetic permeability (μ) of a rock is the measure of how much a rock will react to magnetisation from an applied magnetic field. Again, the MT method assumes a bulk magnetic permeability for a rock and treats magnetic permeability as isotropic and therefore a scalar quantity (Miensopust 2010). The magnetic permeability relates the magnetic intensity (H) and the magnetic induction (B):

$$B = \mu H \tag{3}$$

As a rule, most rocks have a magnetic permeability close to the value of μ_0 (the magnetic permeability in a vacuum; $4\pi \times 10^{-7}$ Vs/Am). Iron-rich rocks have an elevated magnetic permeability which can cause misleading interpretation of MT data in mineralised zones. The Mourne Mountains are not known for their iron-rich rocks and therefore this should not be a problem in this study.

1.3.3. Equations and assumptions of the MT method

MT is an electromagnetic method and is therefore governed by Maxwell's Equations of electromagnetism:

(4) $\nabla \cdot E = \rho / \varepsilon$

(5) $\nabla \times E = -\frac{\partial B}{\partial t}$

(6) $\nabla \cdot B = 0$

(7) $\nabla \times B = \mu J + \mu\varepsilon \, \delta E/\delta t$

Where E = electric field, B = induced magnetic field, ρ = charge density, ε = electrical permittivity, t = time and J = current density.

Maxwell's Equations can be manipulated to derive any electromagnetic field. This is important for calculating the interactions of conductors and resistors and the overall electrical resistivity structure of an area.

When identifying boundary conditions of an electromagnetic field Ohm's Law must be considered:

(8) $J = \sigma E$

By using Ohm's Law and Maxwell's Equations the boundary conditions between different media can be deduced.

The data used within this project only made use of a frequency range of 0.001 – 1000 Hz, thus allowing for the assumption that the source field is quasi-static. A quasi-static field results is when:

(9) $T \gg \varepsilon/\sigma$

Where T = periodicity (1/f), ε = electrical permittivity and σ = conductivity.

The assumption made by the quasi-static field is that the change is so slow that it appears to be a static field, unless the sampling rate is sufficient to record change (high frequency data).

Upon this assumption, only Equations (5) and (7) of the Maxwell's Equations are required and can be simplified to:

(10) $\nabla \times E = -\frac{\partial B}{\partial t}$

(11) $\nabla \times B = \mu\sigma E$

The MT method relies on eight assumptions. These are discussed in detail in various publications (e.g. Cagniard 1953; Simpson & Bahr 2005). Below is a summary of these assumptions (*after* Simpson & Bahr 2005):

i. Maxwell's Equations for electromagnetism are obeyed at all times.
ii. The Earth (rock) does not generate electromagnetic energy. Electromagnetic energy is only dissipated or attenuated.
iii. Away from their source fields all electromagnetic fields are conservative and analytic.
iv. The electromagnetic source field is sufficiently far from the Earth's surface to be treated as a plane wave source.
v. Free charge cannot accumulate to form dipoles. This does not include non-inductive static shifts at conductive discontinuities.
vi. The Earth is an ohmic conductor where charges are conserved (i.e. Ohm's law is obeyed).
vii. Recorded signal is in the range to be classed as a quasi-static field.
viii. Mineralogical variations in electrical permittivity and magnetic permeability in rocks is negligible in comparison to the bulk rock conductivity. The inversion method used neglects the effect of mineral fabrics and their ability to create a electrical or magnetic anisotropy.

1.3.4. Transfer Functions, Apparent Resistivity and Phase

Transfer functions relate the electric and magnetic fields within the recorded MT data at any particular frequency. The Impedance Tensor (Z) describes the relationship between the orthogonal components of both the electric and magnetic fields:

(12) $$\mathrm{Z} = \frac{E}{H}$$

OR

(13) $$E = \mathrm{Z} \times H$$

Z can be then be rewritten in terms of the transfer function matrix:

(14) $$\begin{bmatrix} Ex \\ Ey \end{bmatrix} = \begin{bmatrix} Zxx & Zxy \\ Zyx & Zyy \end{bmatrix} \begin{bmatrix} Hx \\ Hy \end{bmatrix}$$

The impedance tensor consists of four tensor elements, each of which are complex numbers and is represented by a matrix. These complex numbers have real and imaginary components, thus each element in the impedance tensor has a magnitude (i.e. the apparent resistivity) and a phase response.

Apparent resistivity is described by the equation:

$$\rho_{a(xy)}(\omega) = \frac{1}{\omega\mu}\left|\frac{Ex(\omega)}{Hy(\omega)}\right|^2 \quad (15)$$

Phase is described by the equation:

$$\phi_{(xy)}(\omega) = \tan^{-1}\left(\frac{Ex(\omega)}{Hy(\omega)}\right) \quad (16)$$

Both equations (15) and (16) make use of ω, the angular frequency where $\omega = 2\pi f$.

The Magnetic Transfer Function (sometimes informally referred to as the "tipper") relates vertical component of the magnetic field to the horizontal components:

$$Hz = [Tzx \quad Tzy]\begin{bmatrix} Hx \\ Hy \end{bmatrix} \quad (17)$$

The magnetic transfer function is later used to plot induction arrows (see Section 2.4.).

The impedance tensor and the magnetic transfer function are fundamental to the analysis, modelling process and interpretation of MT data.

Another important feature to consider are the terms TM (transverse magnetic) and TE (transverse electric) modes used in 2D modelling. These are two decoupled electromagnetic modes that propagate in two-dimensional electrical (i.e. geological) media, however, these two modes are only applicable where the diagonal components can be reduced to zero.

For 2D modelling the profile must be oriented perpendicular to electrical strike direction, the TM mode has electrical currents flowing perpendicular to strike and the TE mode has electrical currents flowing parallel to strike. The TM mode is therefore running parallel to the modelling profile. Charges build up at boundaries in the TM mode, thus boundaries are much more pronounced in the TM mode compared to the TE.

Data analysis, through use of Groom & Bailey (1989) decomposition and first implemented by McNiece & Jones (2001), attempts to minimise the diagonal elements

of the 2D impedance tensor to zero through a rotation with respect to true north (see Section 2.4). This results in:

(18) $$\begin{bmatrix} 0 & Zxy \\ Zyx & 0 \end{bmatrix} = \begin{bmatrix} 0 & Z_{\mathrm{TE}} \\ Z_{\mathrm{TM}} & 0 \end{bmatrix}$$

The TM and TE mode are by their nature opposite in sign and thus are represented in different quadrants in the phase (Miensopust 2010); they are 180° out of phase.

1.3.5. The RMS error difference

The root meant square (RMS) error difference is an elemental statistical representation of the accuracy of a model calculation with respect to the observed data. It is used during the analysis of data (see Section 2.4) and to test the reliability of a model (see Section 2.5). The RMS error difference is calculated using:

(19) $$\text{RMS error difference} = \sqrt{(d_{obs} - d_{model})^2}$$

In the modelling software WinGLink, RMS errors are 'normalised' by the data errors calculated during data processing. Normalising the RMS error is necessary to establish a fit of the model that matches the observed data to within the existing data errors.

Typically an RMS error of ≤2 is acceptable.

2. Methodology

The MT technique has become almost synonymous with exploring for geothermal reservoirs in the last decade, helping to explore the subsurface electrical resistivity structure of geothermal areas (Uchida 2009). This is largely due to the extremely low resistivity of hot waters and brines in geothermal aquifers in contrast to the surrounding rocks. Furthermore, MT is a cheap geophysical exploration tool which can be used in challenging environments due to its relatively small sized equipment and use of an ambient natural source.

The survey described in this report utilises MT in a slightly different way by aiming to measure the subsurface distribution of highly resistive granite rocks within a relatively conductive Silurian country rock composed of siltstones and mudstones. The MT method has undergone several key developments in the last twenty years, significantly improving data quality through advances in low-noise amplification, GPS synchronisation and automated data acquisition as well as reliable remote reference processing for synchronised data sets (Uchida 2009). Advances in the MT technique have made it an important geophysical exploration tool, applicable to many geological environments. It is a cost effective and highly manoeuvrable method.

2.1. Profile and site selection

The MT survey through the Mourne Mountains was split into three profiles named EMC, WMC and SLA (Fig.2.1.). EMC represents a transect through the eastern magmatic centre, WMC through the western magmatic centre and SLA from Slieveban to Annalong, south of the Mournes. EMC and WMC are oriented to run through the centre of each magmatic centre and are anchored to the same site (wmc019) in the south of the region, running northwards NNE (EMC) and NNW (WMC). The SLA transect was chosen to run south of the mountains aiming to test for the presence of a laccolithic structure as postulated by Stevenson *et al*. (2007) and Stevenson & Bennett (2011).

The nominal site selection was based on an approximate spacing of 1 km along the profiles. Sites were then assessed in the nearby area for the best possible location. The criteria for a good site are (Miensopust 2010):

i. Free from anthropogenic noise. This includes housing, water pumps, electric fencing and power lines.
ii. Adequately sized open space with minimum topography.

iii. The site must have good top soil to bury and protect instruments. Ideally this will have visual cover from roads or residential areas so as not to attract attention.

iv. Be within reasonable proximity to 'ideal' site locality along the profile (some deviation is allowed from the exact profile trace).

Permits were attained from land owners such as local farmers and particularly trustees to a number of parklands in the Mourne Mountains.

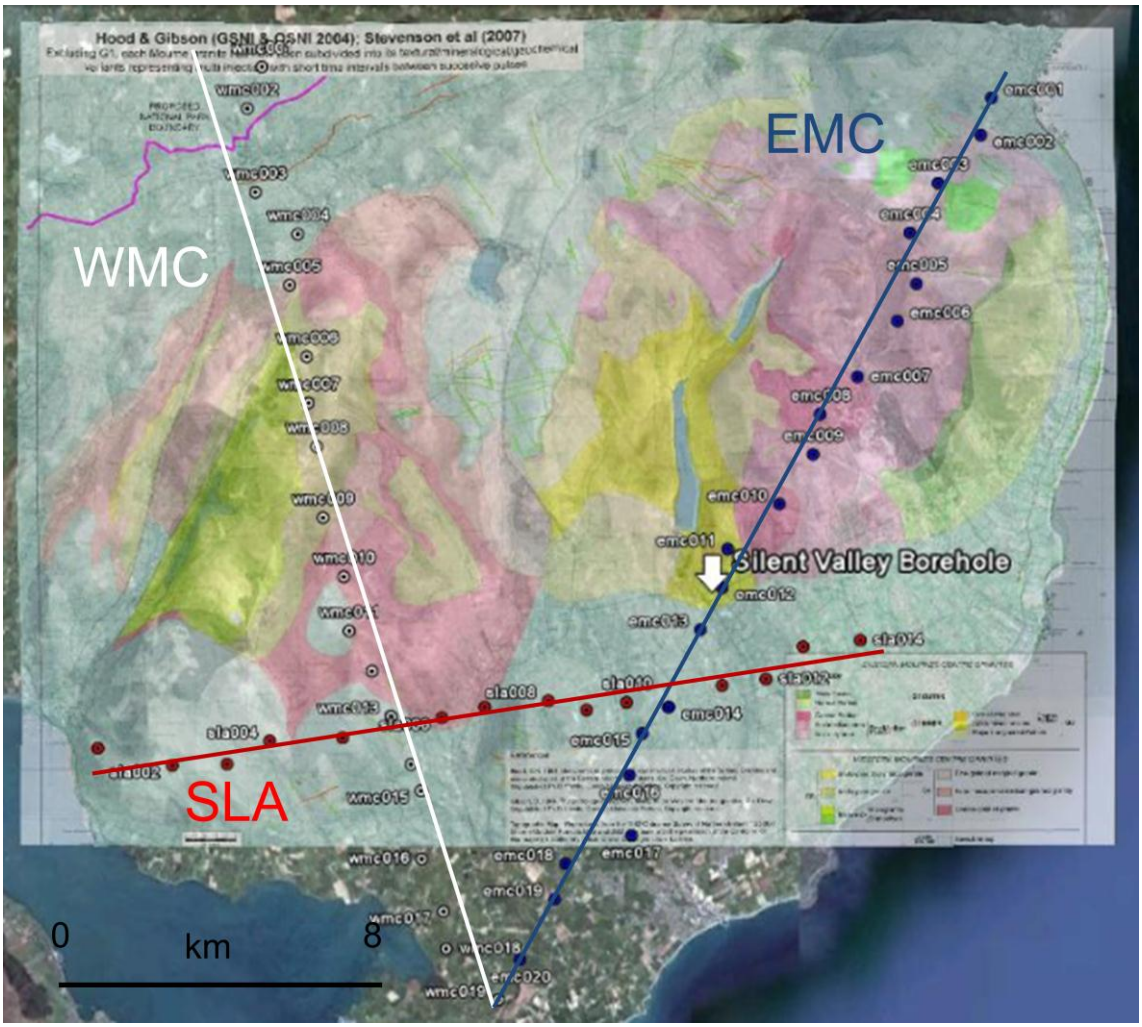

Figure 2.1 GoogleEarth mash-up of the Mourne area with overlain geology and MT site for all three profiles (Hood & Gibson GSNI & OSNI 2004; GoogleEarth 2011)

AMT data were collected at each site with MT data being collected at every other site where possible (occasionally two AMT sites would lie between each MT site due to terrain limitations).

2.2. Data acquisition

To encompass a wide range of frequencies and have a good penetration depth, both MT and AMT data were collected. AMT data are higher frequency than MT data and are sensitive to structures at shallower depth. Both AMT and MT data are collected, processed and analysed in the same way and are integrated for modelling purposes. Thus, when discussing MT it can be assumed this is applicable to AMT unless otherwise noted.

MT data acquisition requires that electrical and magnetic data are recorded simultaneously in order to measure their variation with time. Thus, initial raw data in MT is recorded in the time domain. Electrical data are recorded horizontally in two orthogonal directions (usually oriented north-south and east-west) dubbed E_x and E_y. Magnetic data are recorded similarly, however, a third, vertical, measurement is also included; these are named H_x, H_y and H_z. E_z is not measured as current flow from ground surface to the medium above (air) is almost zero (Tikhonov 1950). The diagram below shows the equipment setup at each site (Fig.2.2.):

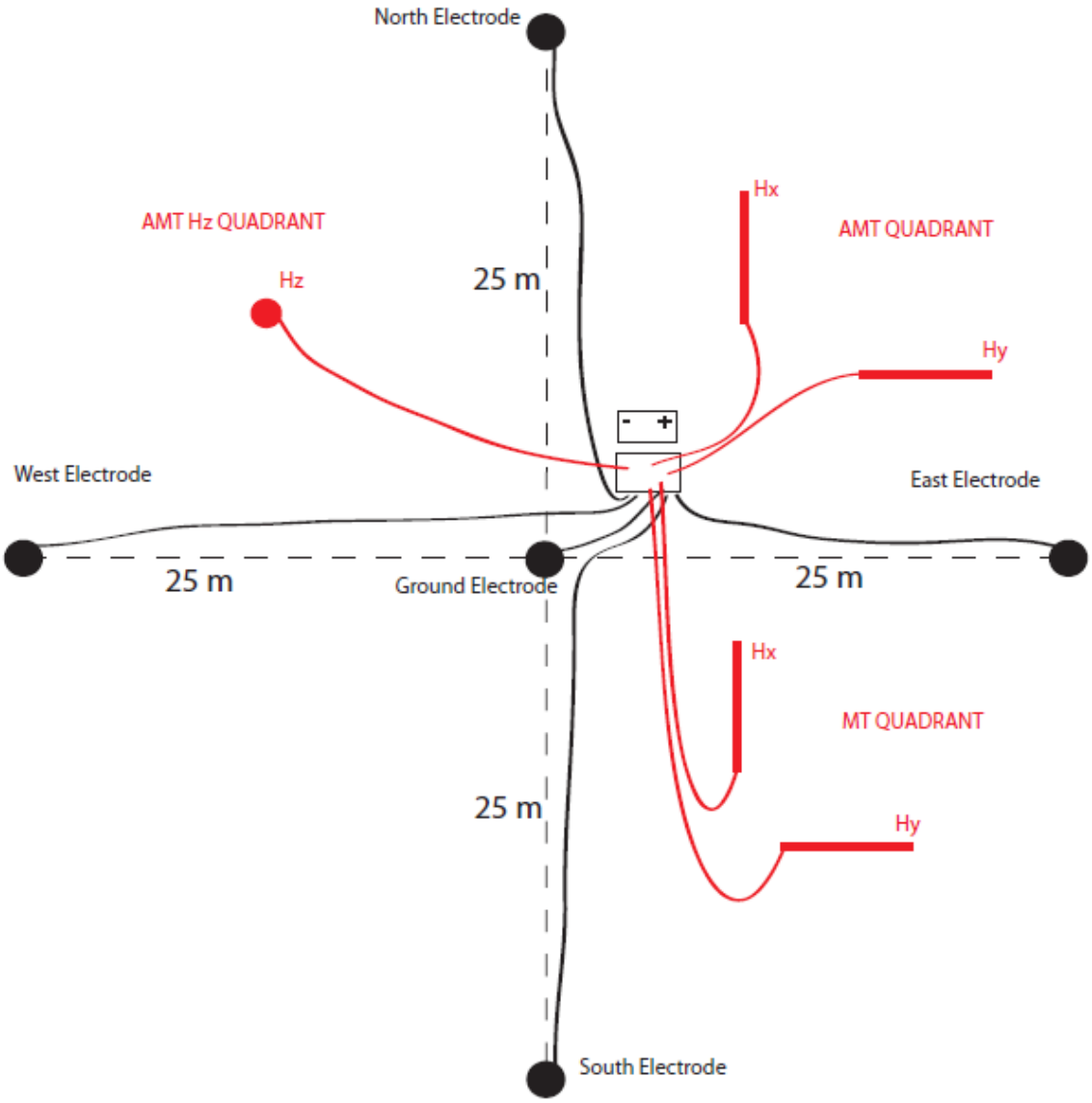

Figure 2.2 Equipment set-up for MT site. For AMT-only sites, the MT QUADRANT is not set-up. The electrodes are set up to create a total 50 m dipole aligned north-south and east-west.

The equipment used during this survey was manufactured by Phoenix Geophysics and included Phoenix Geophysics MTU5 recorders, MTC-30 AMT coils, MTC-50 MT coils and non-polarising electrodes (enclosed lead chloride).

2.2.1. Installation

The site is installed with maximum possible precision. The ground electrode is placed first and then, using a tripod and compass, the north, south, east and west electrodes are aligned accurately with respect to magnetic north. Each electrode is 25 m away from the ground electrode to provide a total 50 m dipole north-south (E_x) and east-west (E_y). A long dipole length is required to minimise electrical noise – particularly poor data were recorded at site emc001 where short dipoles (E_x = 22.7 m; E_y = 34.2 m) was required

due to the size of the site. Electrodes are then buried in the ground at about 20 cm depth. It is important especially in dry soils for a mud to be made in the base of the hole to aid current flow. Good electrical connectivity is achieved by mixing salted water with the soil (on occasion $CuSO_4$ based electrodes were used, in which case $CuSO_4$ solution was mixed with the soil so as not to degrade the electrodes). Following this, all horizontal magnetic coils (magnetometers) are aligned north-south (H_x), east-west (H_y) and then buried to a minimum of 5 cm below the surface and levelled using a spirit level. The vertical magnetometer, H_z, (only recorded in AMT data, apart from site wmc008) is then buried as deep as possible in a separate quadrant to avoid interference with other magnetometer coils and made vertical with a spirit level. All components are connected to the recording box (MTU5 recorder) which is powered by a 12V car battery. Resistance and voltage along the electric dipoles is measured. Resistance and voltage measurements define the level of low-pass filtering that should be applied to the raw data. A low resistance would require a strong low-pass filter, and *vice versa* for a high resistance.

The MTU5 recorder includes a GPS to find co-ordinates for the site as well as elevation and also allows for synchronised data recording between sites. Synchronicity between sites is essential for later processing which make use of remote reference methods. Examples of field sheets used at each site to record key details are given in Appendix I.

2.3. Data processing

Data processing is a fundamental part of the magnetotelluric method. Raw field data are collected in time series. It is necessary to produce MT transfer functions (e.g. detailed by Jones *et al*. (1989)) from raw time series data. This is achieved through a three step process involving preconditioning of the data, conversion of time series data into the frequency domain and estimation of the transfer functions (Miensopust 2010).

Preconditioning the data essentially involves removal of large spikes in the data which represent severe, short-lived noise. A second part of preconditioning is the partitioning of the time series data into many time segments of equal length. Longer recording periods will result in more segments and will provide more statistically robust results (Miensopust 2010).

Due to the segmentation of the time series applying a Fourier Transform would result in spectral distortion of the data and thus a window function is applied to the time

segments (Miensopust 2010). The window function then allows a discrete or fast Fourier Transform to convert the segmented time series into the frequency domain. Data can now be calibrated to the instruments specific sensitivity using the field calibration files which are frequency dependent for magnetic induction coils (Miensopust 2010). Calibration is essential to remove the instrument frequency response to reveal the Earth's frequency response.

Once transformed into the frequency domain and calibrated, the data can be examined in terms of its magnetic and electric fields for each time segment through a Spectral Matrix (Miensopust 2010). Spectral matrices are then stacked and edited or weighted using statistical techniques for each frequency (Miensopust 2010).

Following this, the MT transfer functions can be estimated, represented by the impedance tensor (Z; based on both the electric and magnetic fields) and the tipper (the vertical magnetic field; H_z) with respect to the horizontal magnetic fields (H_x and H_y). See Section 1.3 for more details on the impedance tensor and tipper vector.

The transfer functions have unavoidable errors built in to the calculation due to background noise, particularly electrical, distorting the geological signal (Simpson & Bahr 2005). Errors take the form of statistical and biased errors in the transfer functions. Errors can be estimated and can be reduced. Statistical errors are discussed in detail by Jones *et al*. (1989) and can be reduced by analysing more data or using more robust processing methods. Bias errors are examined by Sims *et al*. (1971) who suggest a mean is taken to minimise bias, however, Gamble *et al*. (1979) introduced remote reference processing. Remote reference processing compares the 'local' magnetic field (recorded at the site in question) with that of a 'remote' site (away from the local which recorded data simultaneously) to allow retention of good correlated signal and rejection of uncorrelated signal. It is general practice to use the horizontal magnetic fields as part of remote reference processing as these do not suffer from the effects of anthropogenic electrical noise and are therefore least biased and statistically the best choice (Miensopust 2010). The remote reference processing method avoids biased errors by comparing simultaneously recorded data to remove noise-induced bias. Despite this, remote reference processing actually increases the statistical error for a particular site (Jones *et al*. 1989) through the increase in size of error bars but the final calculated MT responses are more robustly determined.

Data processing in this project was done using Phoenix Geophysics software (SSMT2000) which makes use of robust cascade decimation by Jones & Jödicke (1984) (method 6 in Jones *et al*. (1989)) for local (single site) and remote reference processing. This method is not as intensive as other more thorough robust methods but can be applied in the field effectively as it uses relatively few computations (Jones *et al*. 1989).

Once processed, the partial responses (the result of the earlier segmentation) can be further edited manually to remove any residual noise in the data. The partial responses each have a calculated MT response and it is a comparison of these MT responses for each time segment with anomalous MT responses rejected. This type of editing is done using Phoenix Geophysics software (MT Editor).

Following this the data must be rotated to true north as the field data is collected with respect to magnetic north. Rotating the data to true north is important later when analysing for geoelectrical strike direction and the resistivity structure of the area.

The final phase of data processing is to stitch AMT and MT data strands together so that they can be analysed and modelled simultaneously. This is done by identifying a cross over in the two data sets (usually toward the long-period end of the AMT data range) and using a program to amalgamate the two data sets. This can lead to a step in the data along the apparent resistivity curve, however this is often always minor. A step in the data is negligible if the steps are smaller than the error floors imposed during the 2D inversion modelling (see Section 2.5.2.). Appendix II shows plots of stitched data with small steps identified.

2.4. Data analysis

Once data processing and editing is complete and data sets for each site for both phase and resistivity appear satisfactory it is important to analyse the data in terms of geoelectrical strike direction and data dimensionality.

Data dimensionality is a description of the overall electrical resistivity structure of the area and how currents flow in response to that structure:

- 1D: horizontally layered structure, where electrical resistivity only varies vertically (Fig.2.3.).

- 2D: dipping layered structure with a dominant regional geoelectrical strike direction. Electrical resistivity varies perpendicular to strike but not parallel to strike (Fig.2.3.).
- 3D: electrical resistivity varies in three dimensions, laterally and vertically.

Dimensionality can often be inferred by the shapes of the apparent resistivity curves and if the XY and YX modes (the TE and TM modes in two dimensions) diverge. It is difficult to identify a specific strike direction from the shapes of the curves alone although it is quite straight forward to distinguish between a 1D structure, where the XY and YX modes are very similar, and a 2D structure where the XY (TE) and YX (TM) modes diverge. It is possible to get 1D and 2D structure in the same data set at different sites, or at the same site at different depths. When identifying a 2D structure, the Z_{xx} component of the impedance tensor is reduced to approximately zero where Z_{xy} is maximised. In 3D, Z_{xx} can never be zero.

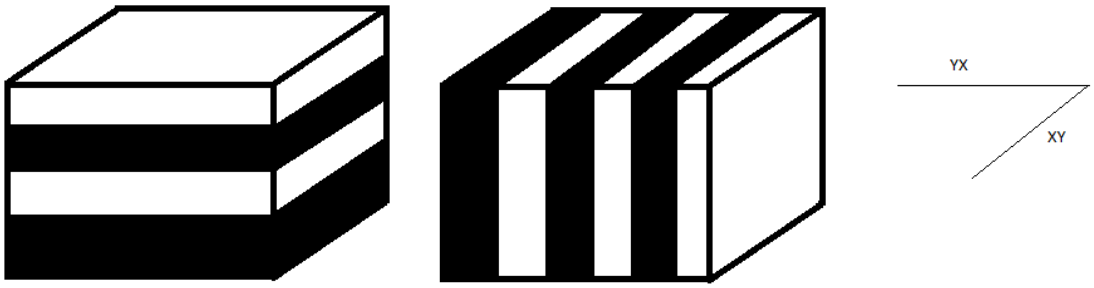

Figure 2.3 Left: 1D geological setting for a horizontally layered medium where XY and YX currents will be similar and only vary with depth. Right: 2D, vertically layered medium where XY (TE) and YX (TM) vary laterally but are assumed to be continuous perpendicular to YX (TM).

Data analysis was undertaken at Dublin Institute for Advanced Studies where UNIX computer code was used to identify favourable strike direction within the range 0-90° to produce a strike sensitivity plot. Plots can also be produced in map form based on phase difference, RMS error and electrical strike direction to show regional and local variations as well as identify sites that are 1D (no specific current flow and electrical strike direction) and sites that are 2D (a strong current flow perpendicular and parallel to electrical strike direction and high phase difference). Identifying a preferred geoelectrical strike direction for the whole profile is done using the Groom & Bailey 'model' where Groom & Bailey (1989) decomposition is used to identify the best azimuth where diagonal components of the impedance tensor are minimised.

A strike sensitivity plot finds the most favourable angle of rotation for a site based on the RMS error calculated for every possible angle between 0-90° and compares these to

all other sites. The strike sensitivity plot allows for comparison across a profile and gives an idea of overall orientation or a regional geoelectrical strike direction as well as for individual sites.

Further analysis can be done using WinGLink software to produce polarisation maps at specific frequencies to analyse the data with both resistivity and tipper data (induction arrows; see Section 1.3.4.) on the same plot. This provides a good visual aid but does not provide a quantitative value for geoelectrical strike.

It is important to consider both electrical and magnetic data when determining geoelectrical strike, however, the use of the magnetic field with use of the tipper provides a direction of current flow and a strike that is free from electrical noise. The tipper is an important feature to consider when deciding on the orientation of geoelectrical strike in the area. The tipper strike is also not subject to the 90 ° ambiguity that exists in electrical data. For the electrical data alone, in the absence of an obvious geological strike direction, it is not clear which direction corresponds with current flow perpendicular to strike (i.e. TM) and which corresponds with flow parallel to strike (i.e. TE). Examples of these different data analyses are given in Appendix III.

From analysis of the data it was deemed each of the profiles had a preferred strike orientation as follows:

EMC: 72°
WMC: 34°
SLA: 30°

To align the profiles to these strike directions requires decomposition of the data using Groom & Bailey (1989). Decomposition using the Groom & Bailey method allows for removal of localised 3D anomalies in the electrical field in the immediate vicinity of the MT site. The basis of the method results in a rotation matrix, a distortion matrix and a scaled 2D impedance tensor. Groom & Bailey decomposition allows for 3D distortion to be identified and separated from the regional 1D or 2D response (Miensopust 2010). Distortion is important to account for as local electrical distortions can be more dominant over a wide range of periods than the regional strike direction (Jones & Groom 1993). It is a requirement when decomposing the data to geoelectrical strike that the TE mode is rotated parallel to strike. This requirement may involve a further 90° rotation of the data during decomposition to facilitate the alignment of TE to the

geoelectrical strike direction in the case of determining the 90° ambiguity seen in electrical data. Once the data is decomposed to geoelectrical strike, accurate 1D and 2D modelling can be done along the profile.

2.5. Inversion Modelling

Before numerical inversion modelling can be undertaken, the decomposed data must be checked for D^+ consistency after Parker (1980; 1982) and Parker and Whaler (1981). This is a 1D test on the consistency of the apparent resistivity and the phase through the use of the 'c' function – the admittance (Miensopust 2010). The method is able to calculate a basic 1D model using apparent resistivity, phase, or both and give guidance when selecting bad data points. It is common to further edit data before full modelling by masking noisy and D^+ inconsistent data in WinGLink and the D^+ method is built into the software package. All modelling is done using WinGLink software.

2.5.1. 1D inversion

1D modelling involves creating an 'Occam model' which allows the observed data to be modelled in terms of depth with respect to the apparent resistivity. The Occam model is comprised of a maximum of 43 layers that model resistivity variation with respect to depth and compare this to the observed apparent resistivity and phase responses. The Occam model inversion can be based on the TM, TE or the invariant (average of both TM and TE). 1D modelling for this survey was done using the invariant so as not to bias for one particular mode. The resistivity model produced by the Occam method is just one approach to 1D modelling using WinGLink software. A second method using an 8-layer model can then be used to estimate changes in resistivity with sharp boundaries rather than the comparatively smooth Occam method. Both approaches are equally valid providing the modelled responses fit the observed data. The Occam model is calculated first and subsequently used to guess a starting model for the 'sharp-boundary' inversion model. These approaches give an approximate model to account for changes in resistivity with depth (1D) in a layered Earth model.

From these estimated layered models an overall profile model can be created through smoothing between sites. The 1D model is also useful for estimating the depth of penetration for each site which helps to know at what depth structures can accurately be constrained.

2.5.2. 2D inversion

Smooth 2D numerical inversion was undertaken for all three profiles in the survey. 2D inversion allows for the modelling of resistivity in terms of depth and for changes laterally along the profile. 2D inversion models for the observed TE and TM modes as well as the observed tipper data simultaneously for all sites along the profile.

The first stage of 2D inversion is to create a forward model for a starting model with a 100 Ω.m apparent resistivity (apart from those designated as sea water; 1 Ω.m). The forward model calculates for the whole model, the apparent resistivity, phase and tipper using the observed data and Maxwell's Equations. The result of this is to produce a calculated resistivity curve, phase and tipper for each site incorporating effects of the whole model using the initial data. This is compared to the observed data through the RMS error. The first forward model makes use of the starting model and thus a comparison between observed data and a near homogenous medium has a high RMS error. After a forward model has been calculated the process of changing the model to achieve a better RMS error is carried out; this is the inversion process.

The inversion 'work flow' is an important part of 2D modelling. It is the steps that follow that shape the final model which can have fundamental consequences on the final results.

Before modelling in 2D a satisfactory mesh of cells must be created and then the inversion smoothing factors must be tested to ensure minimum bias when producing the final smooth model. Smoothing is controlled by three variables, tau (the overall smoothing factor), alpha (the horizontal smoothing factor) and beta (the vertical smoothing factor). Initially the mesh is tested in terms of tau only. This is done by running several inversions models on the mesh with a homogenous 100 Ω.m fill. The RMS error can then be plotted up as follows (Fig.2.4.):

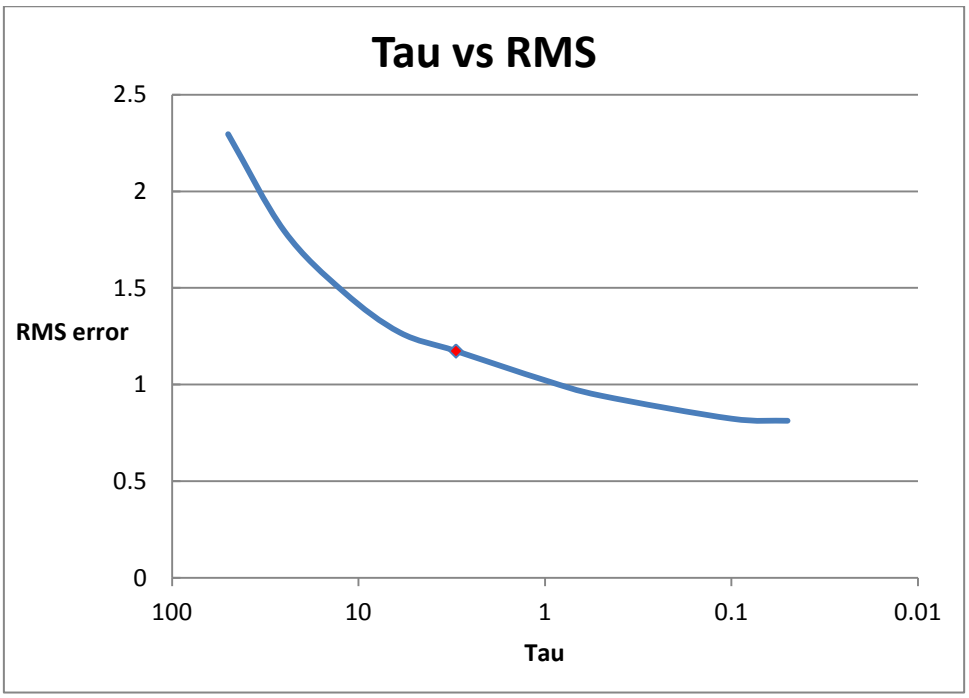

Figure 2.4 Plot of tau versus RMS values.

A tau value of 3 was chosen as this is closest to the inflection point on the logarithmic scale between the upper, steep portion and the lower, shallow portion where decreasing the tau value has little effect. If the calculated model for a tau value of 3 appears to have a horizontal or vertical bias in the model (usually an artefact of the mesh) this can be accounted for by modifying alpha and beta. Horizontal and vertical bias is tested for in the same way as tau, but with tau fixed, and can generally be judged by eye to create the best geologically aesthetic model. The final smoothing parameters decided up for all three profiles are:

Tau: 3
Alpha: 2
Beta: 0.5

Once satisfactory smoothing factors have been identified, full inversion modelling can begin. The same smoothing factors were used for all models by creating a similar mesh for each profile.

When creating a 2D inversion model, each particular constraint that can be applied to the model (apparent resistivity, phase and tipper) are introduced with an error floor. WinGLink makes use of an inversion algorithm based on Rodi & Mackie (2001) which tries to produce a model to match observed MT data to within their errors, data with

high errors therefore have less effect on the inversion due to a lower weighting. Error floors are introduced to control the weighting of each data element.

The steps used to produce a final inversion model for all three profiles are detailed below:

- Introduce tipper
- Introduce phase (10% error floor) and apparent resistivity (TM and TE at 50% error floor)
- Reduce phase (5% error floor)
- Reduce apparent resistivity (TM at 25% and TE at 50% error floor)
- Reduce apparent resistivity (TM at 10% and TE at 50% error floor)
- Reduce apparent resistivity (TM at 10% and TE at 25% error floor)

Reducing the error floor on the TE mode past 25% resulted in breakdown of the model and saturation of many cells to very high apparent resistivities (see Section 2.5.3.). It has been suggested by Jones (2011, *Pers. Comm.*) that by introducing the tipper first, the model may be biased by small scale conductive features. Modelling has however also been conducted where the tipper is introduced last, this results in an almost identical model but has a higher resulting RMS error. Therefore, the steps as detailed above, were decided would create the best model.

2.5.3. The effects of bathymetry and topography on the 2D model

Accounting for bathymetry

Accounting for the bathymetry is important particularly due to the existence of sea water filling the bathymetric topography. Sea water is an excellent conductor and this has consequences along the profile due to its strong effects on the TM mode. To test to see if sea water needed to be accounted for, a forward model was created with a completely homogenous base model of 100 Ω.m. The forward model MT response data were then saved over the observed data (to become the 'new' observed data) and sea water was introduced into the model with a value of 1 Ω.m. The forward model was re-run and the results showed a strong deviation in the forward model response with respect to the 'new' observed data (i.e. the forward model with no sea was significantly different to the model containing sea water). Thus, sea water must be included in the final model to produce an accurate model.

Topography

The topographic effects in the Mourne Mountains are quite profound and have strong effects in the models. This is primarily due to the quite steep nature of many of the mountains and valleys. The resulting effect on the model is that a fine mesh was required to minimise topographic effects on the TM mode. It is almost impossible to stop the potential effects on the TE mode as the 2D model does not account for features in this direction (perpendicular to the profile), although they will still have an effect on the observed data. The assumption when modelling in two dimensions is that the resistivity features in the cross-section extend to infinity in both directions perpendicular to the profile (i.e. along the TE mode), the same assumption is made in terms of topography. In reality, topography will change perpendicular to the profile and therefore these effects cannot be captured and modelled in a 2D inversion model. To mitigate against the effects of the TE mode it is necessary to include an elevated error floor in the model, an elevated error floor will avoid topographic effects feeding back into the subsurface model (see Section 2.5.2.).

2.6. Heat flow, heat production and temperature calculations

Calculations to determine the heat flow, heat production and temperature at depth are undertaken independently within this report. The data used is a combination of pre-existing data from the Northern Irish TELLUS project (see van Dam 2007), Geothermal Energy Resource Map of Ireland (see Goodman *et al.* 2004), Deep Geothermal Exploration Drilling Programme Completion Report (see Kelly 2010) and data from core tests on samples from the Silent Valley borehole undertaken by Hot Dry Rocks Pty Ltd (see Antriasian 2010).

Equation (1) was used to define heat flow. Below are the two equations used to calculate heat production (20) and extrapolated temperature at depth (21):

(20) $$A = 10^{-5} \times \rho\,(9.52U + 2.56Th + 3.48K)$$

(21) $$T_{ze} = T_{zb} + \left[\frac{(Z_e - Z_b)}{1000} \times \frac{\Delta T}{\Delta z}\right]$$

Where ρ = density, U = uranium concentration, Th = thorium concentration, K = potassium concentration, T_{ze} = Temperature at an extrapolated depth, T_{zb} = bottom-hole temperature, Z_e = depth extrapolated to, Z_b = bottom-hole depth.

These equations are appropriate for a one layer model (e.g. Mourne granite). In a one layer model it is reasonable to assume that A and k are constant throughout the granite. The use of the Mourne Granite Complex as a single layer model is an assumption to idealise the bulk granite for use in the calculation. Both textural and compositional variations between the different facies are well documented (see Hood 1981; Gibson 1984; Cooper & Johnston 2004).

3. Results

Both 1D and 2D modelling results are presented below, followed by heat flow, heat production and temperature calculations relating to the Silent Valley borehole. See Appendix IV for full modelling details and data used in WinGLink.

3.1. 1D modelling results

1D modelling results, although not fully representative of the complexity in the MT data are a useful tool. When modelling the invariant (the average of the TM and TE modes), it is possible to get an overview of how the subsurface model will look before 2D modelling (the 1D model for SLA is a particularly good example of this). 1D models are also useful for estimating the depth of penetration of the data based on the general resistivity or conductivity recorded in the data.

Below are the results of 1D modelling for a 43 layered Occam model followed by estimated layer thickness and apparent resistivity on all three profiles; EMC (Fig.3.1.); WMC (Fig.3.2.); SLA (Fig.3.3.).

3.1.1. EMC 1D model

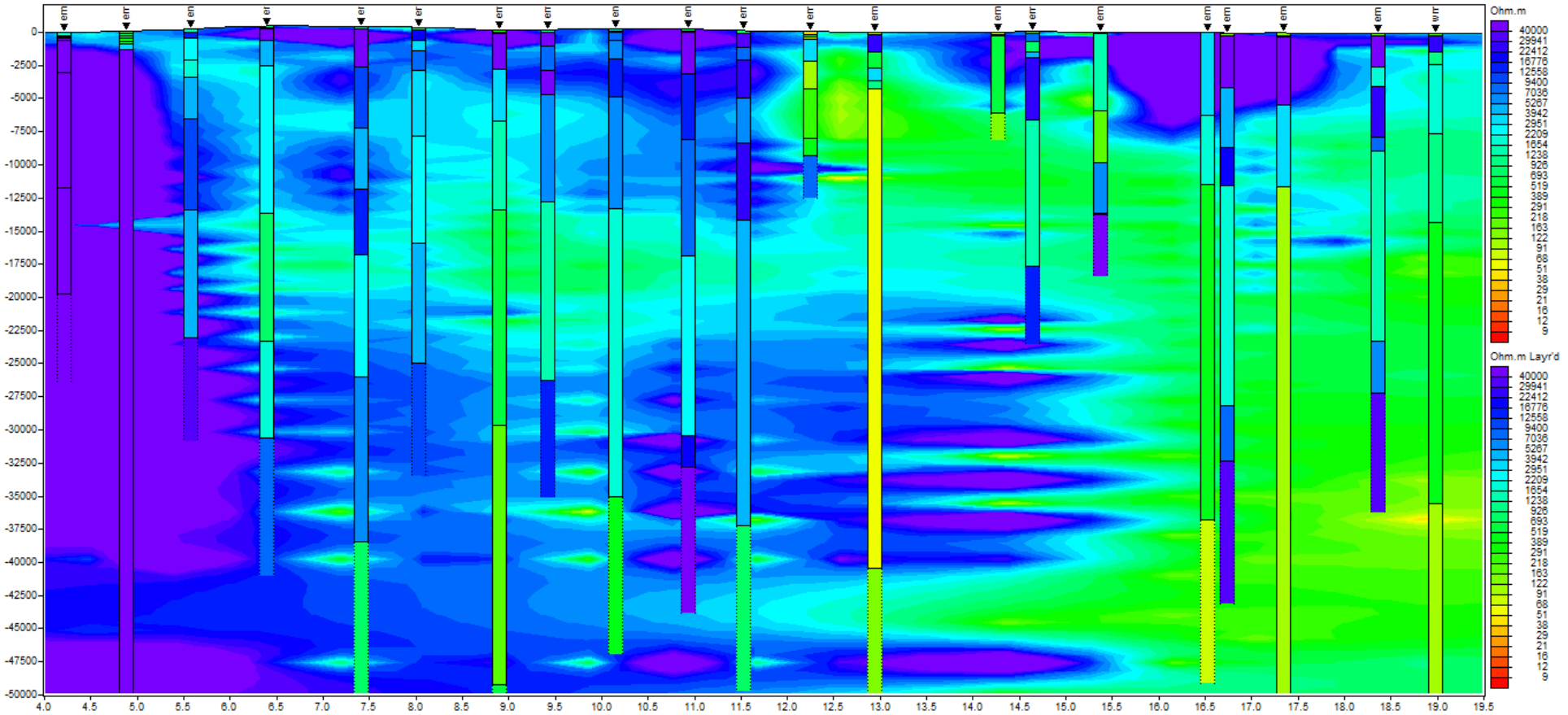

Figure 3.1 1D model of profile EMC with 1D soundings included to show depth of penetration. The EMC 1D model was the first profile to be completed in the survey, and the timing corresponded with a solar flare hitting the Earth and heightened interactions of the solar wind with the ionosphere. The recorded data are of a good to high quality with excellent penetration due to the strong signal. The 1D model shows that resistors may be present at depth and extend southwards below the country rock.

3.1.2. WMC 1D model

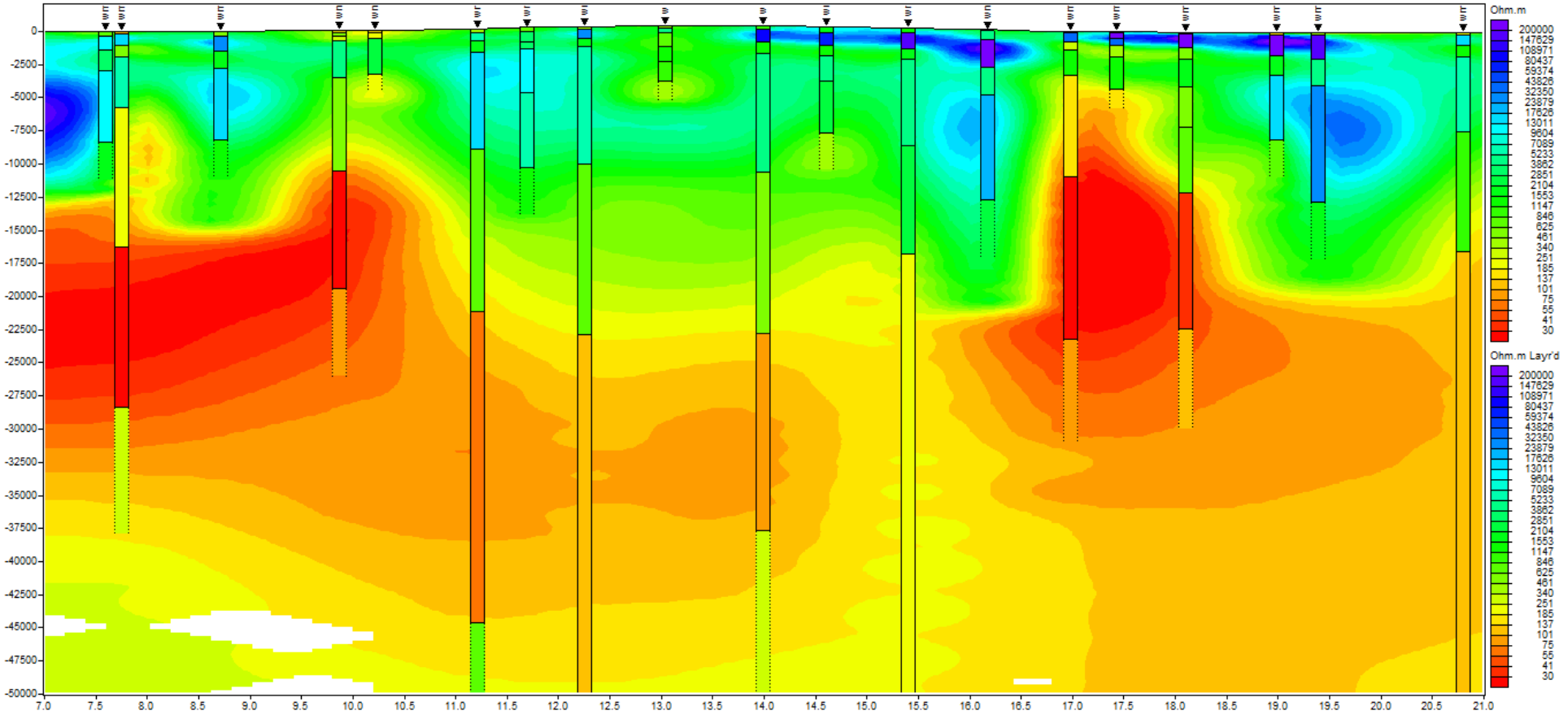

Figure 3.2 1D model of profile WMC with 1D soundings included to show depth of penetration. The WMC 1D model has notably less penetration than that of EMC. AMT recording sites generally have much poorer penetration depths and in places this corresponds with poor quality data. Poor depth of penetration means that many sites can only constrain structure to 10,000 m or less. Thus, deeper structures rely on MT data.

3.1.3. SLA 1D model

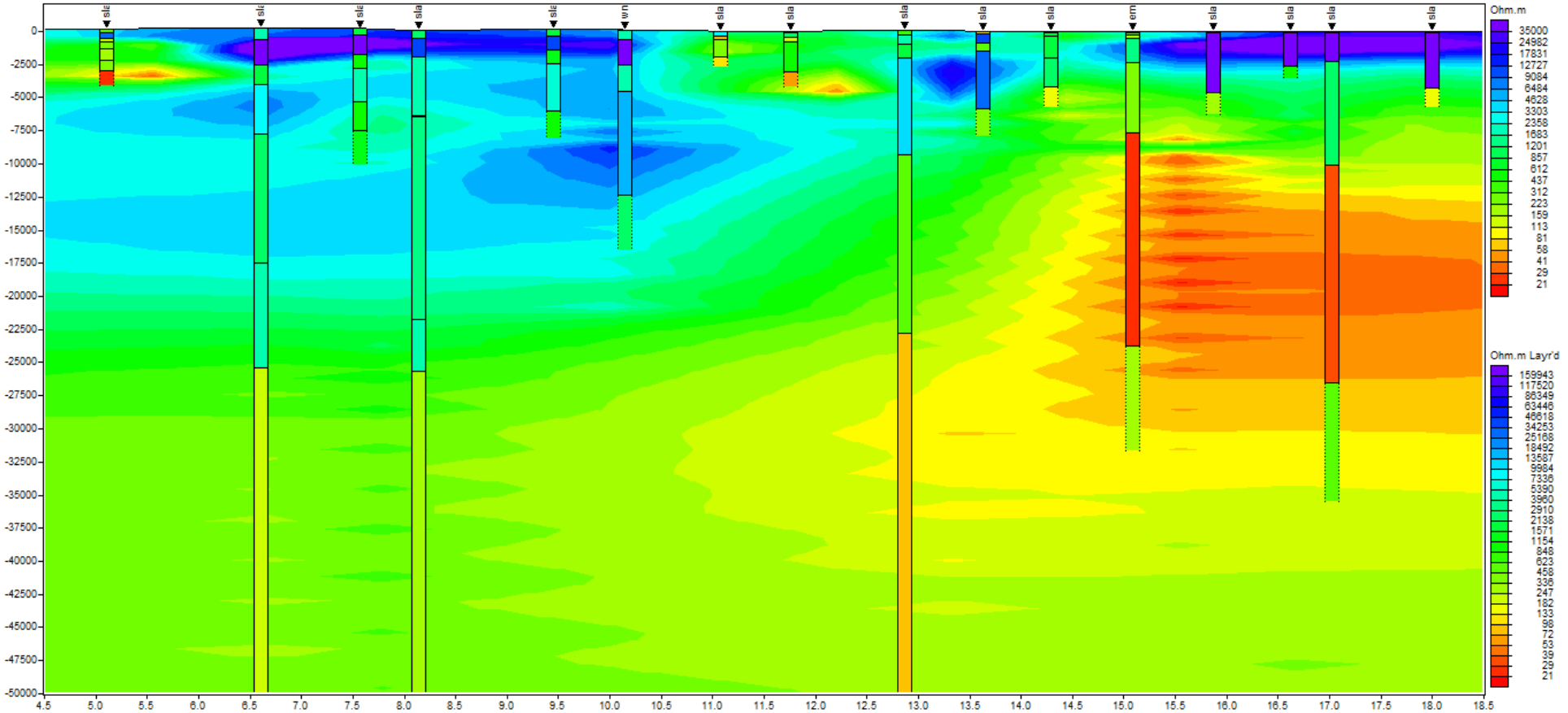

Figure 3.3 1D model of profile SLA with 1D soundings included to show depth of penetration. Data along the SLA profile has a particularly poor penetration depth. This means deeper structures >5,000 m depth will be difficult to constrain. Despite this comparatively poor penetration depth, it is still reasonable to consider the model as current geothermal targets do not lie at depths greater than 5,000 m due to the cost of drilling.

3.2. 2D modelling results

2D modelling of the data was undertaken in WinGLink. The final model parameters used are as follows:

- Smoothing factors: tau = 3, alpha = 2 and beta = 0.5.
- Data range: TM and TE minimum frequency of 0.001 Hz and seven data decades (i.e. up to 10,000 Hz), H_z minimum frequency 0.01 Hz and four data decades (i.e. up to 100 Hz; AMT tipper data only)
- Data used include data errors that have been calculated during data processing and decomposition.
- Error floor: final modelling used error floors of 5% for both TM and TE phase, 10% for TM apparent resistivity and 25% for TE apparent resistivity.
- Station data used (not interpolated data).

The models were started with a bulk resistivity of 100 Ω.m, with the exception of areas of sea water (1 Ω.m). Starting inversions had initial error floors of 10% for phase and 50% for apparent resistivity which were gradually reduced to final parameters.

Presented below are the 2D models for the three profiles; EMC (Fig.3.4.); WMC (Fig.3.5.); SLA (Fig.3.6.).

3.2.1. EMC 2D model

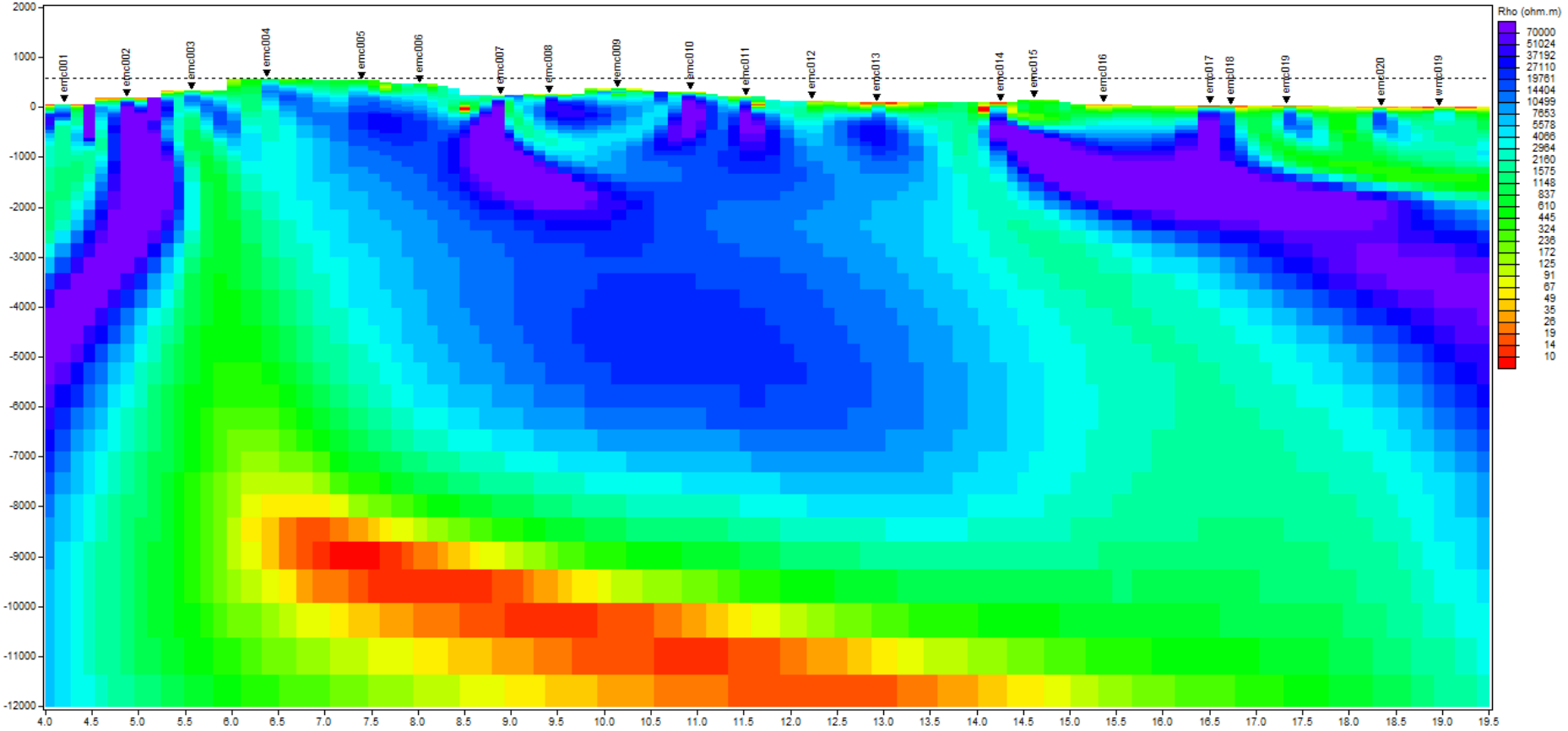

Figure 3.4 2D model of profile EMC. The 2D model for the EMC profile has a reasonable RMS value of 3.2351. Although this is higher than the target RMS of 2, it can be said that the model is quite reliable. The overall RMS error is elevated due to sites emc001 (RMS = 9.4484), emc002 (RMS = 4.7064), emc007 (RMS = 4.5189) and emc008 (RMS = 4.8316). Sites emc001 and emc002 are associated with poor data quality, whereas sites emc007 and emc008 are strongly affected by static shifts in the TE mode.

3.2.2. WMC 2D model

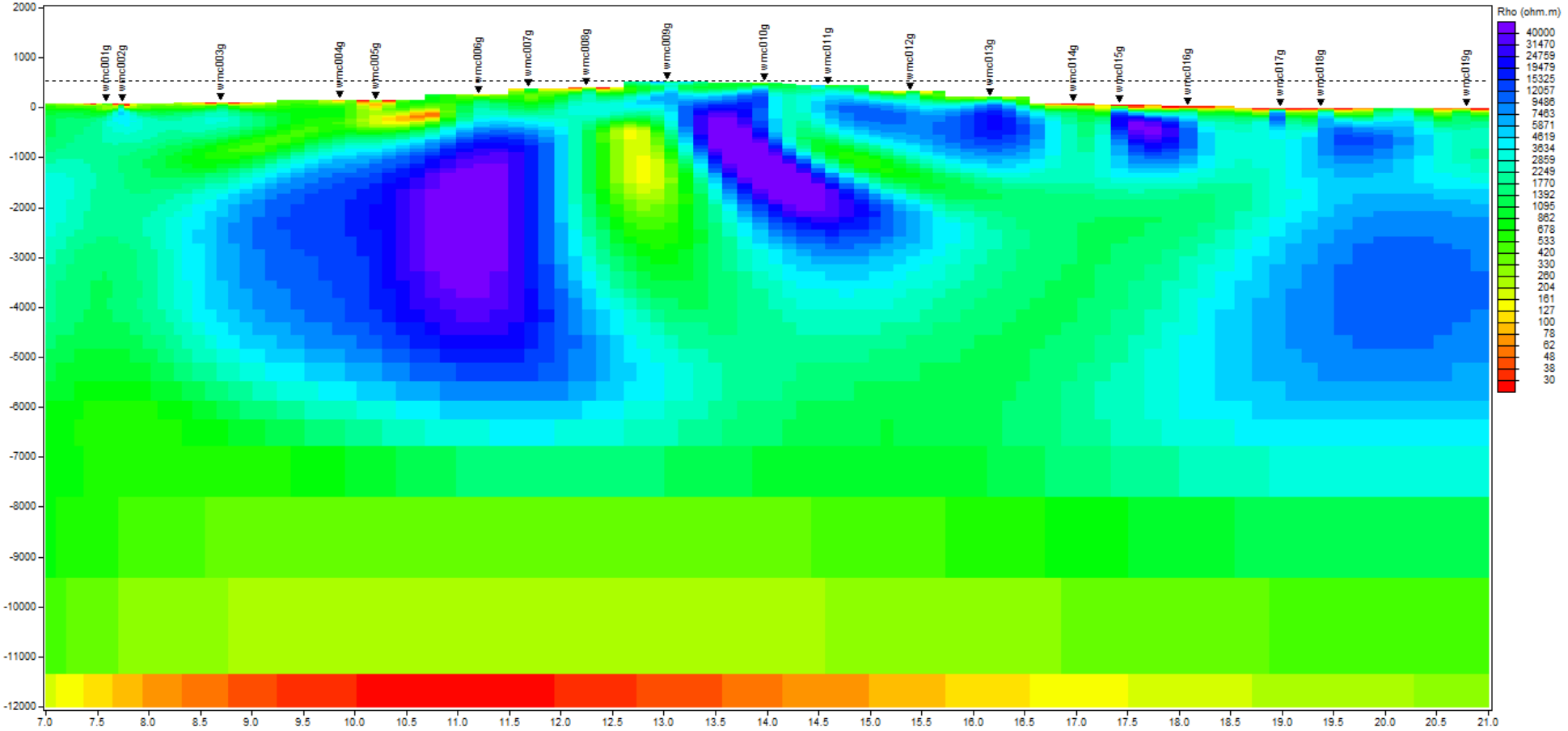

Figure 3.5 2D model of profile WMC. Profile WMC has a good RMS value of 2.01 indicating that the model is very reliable. Individual site RMS values are reasonably constant in the range of 0.9714 to 2.8255; apart from wmc018 (RMS = 4.2843) which is strongly affected by static shift in the TE mode.

3.2.3. SLA 2D model

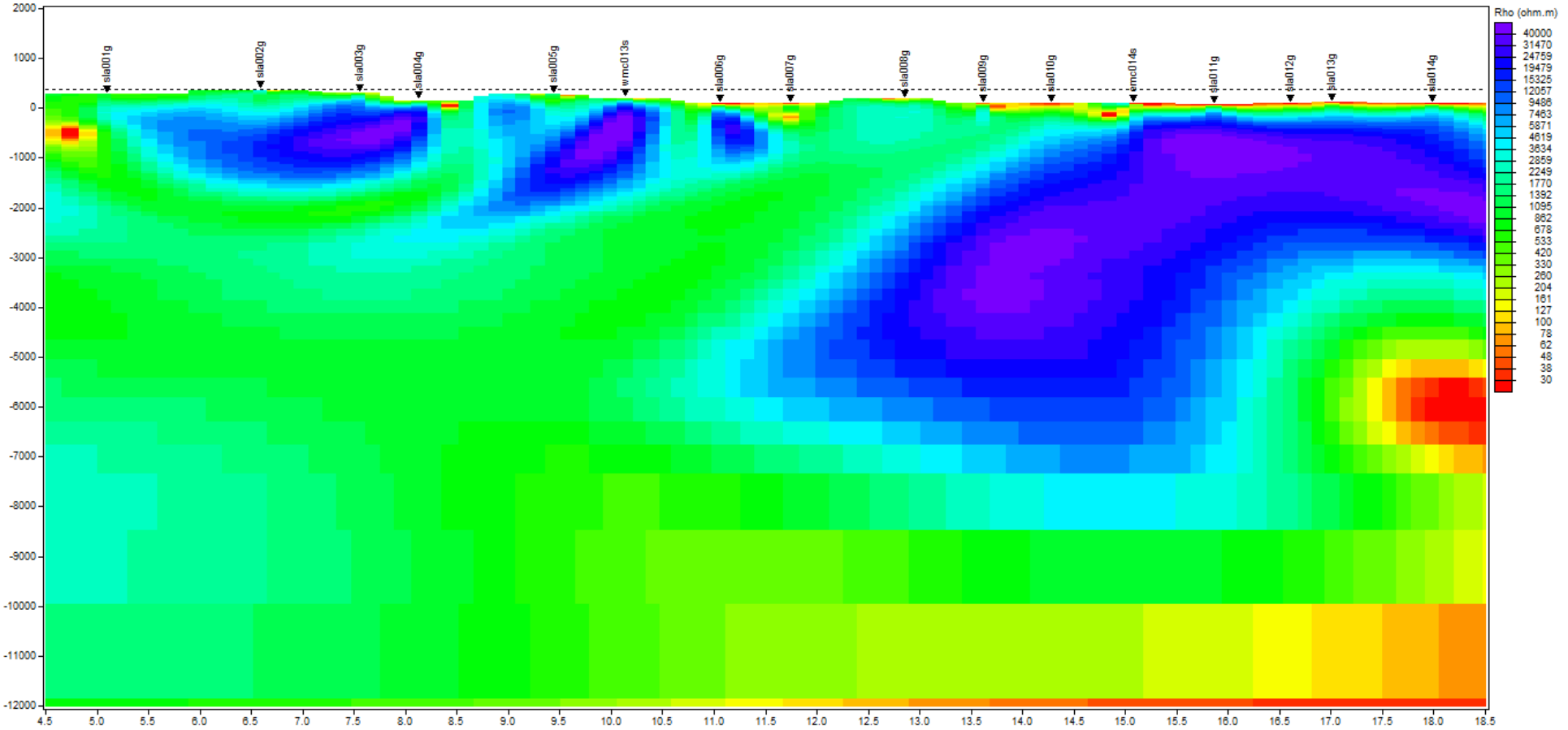

Figure 3.6 2D model of profile SLA. The SLA model has an RMS error of 2.571 and indicates a good reliability. Individual site RMS values are again reasonably constant within the range of 0.9823 to 4.0043. Elevated values occur at sites sla001, sla002, sla004, sla008 and emc014; these are all associated with strong static shifts in the TE mode.

3.3. Geothermal calculations

Data for the calculating heat flow, heat production and temperature were collated from Kelly (2010) and Antriasian (2010). X-ray fluorescence data (Reay 2011) are used for radiogenic isotope concentrations.

Thermal conductivity (k) values for the Mourne granites were taken from Antriasian (2010). Borehole data for the Mourne area comes from the Silent Valley borehole comprised of three samples all from the 'G2' granite facies. The average and standard deviation were taken for all three samples (each tested three times) to calculate the thermal conductivity of 'G2' ($k = 3.48$ W m^{-1} K^{-1} ± 0.09). Density (ρ) was only measured from one sample, this was done three times and the average and standard deviation calculated ($\rho = 2.594$ g cm^{-3} ± 2.08).

A bottom-hole temperature is provided by Kelly (2010) of 21.861 °C at 591 m depth. The geothermal gradient is also taken from Kelly (2010). Given as 21.07 °C/km, this has been calculated using a temperature change (ΔT) of 11.608 °C (21.861 °C – 10.253 °C) over a depth range (Δz) of 551 m (591 m – 40 m).

3.3.1. Heat Flow

Heat flow is a function of the geothermal gradient and the thermal conductivity of the host rocks (Equation 1).

$$Q = 3.48 \times \frac{11.608}{0.551}$$

$$Q = 73.31 \text{ mW m}^{-2}$$

The thermal conductivity is assumed in this work to be constant throughout the Mourne Granite Complex, despite known textural and mineralogical variations between facies. In practice, more sampling of the granite facies could reveal that the different facies have variable thermal conductivities. The thermal conductivity is average from three samples of the 'G2' granite facies (Antriasian 2010; Kelly 2010).

The geothermal gradient used is an average for the Silent Valley borehole and is sampled over quite a short depth range. Not only is the geothermal gradient measured at shallow levels, it is assumed in this work that the geothermal gradient is constant and does not change with depth.

3.3.2. Heat Production

The radiogenic heat production calculation (Equation 20) takes into account radiogenic element concentrations (see Reay 2011) and density (see Antriasian 2010) and empirically derived constants relating to the heat production through radioactive decay. The calculation used is from Rybach (1988). The author recognises that the equation used is not the most up-to-date and that equations by Carmichael (1989) exist with perhaps more accurate constants for radiogenic heat production for each isotope (see van Dam 2007). However, access to the original equations by Carmichael (1989) is limited and equations in van Dam (2007) are not fully presented and do not define the density used in the calculation. Thus, Rybach's equation will be used and compared to calculations by van Dam (2007) and Reay (2011) (Fig. 3.7.).

	Calculated using Rybach (1988)					Calculated by Reay (2011)				
Sample	**G1**	**G2**	**G4**	**G5**	**Total**	**G1**	**G2**	**G4**	**G5**	**Total**
1	3.69	4.50	5.99	5.02		3.71	4.53	6.04	5.05	
2		14.50	6.19	5.04			14.64	6.24	5.08	
3		10.16	5.72	6.8			10.25	5.76	6.85	
4		8.87		7.79			8.94		7.85	
5		6.24					6.29			
6		6.31					6.36			
7		5.98					6.02			
8		7.23					7.29			
9		6.68					6.73			
10		6.56					6.61			
11		4.85					4.88			
12		5.7					5.75			
13		6.19					6.23			
Average	3.69	7.21	5.9667	6.1625	6.44	3.71	7.2708	6.0133	6.2075	6.49
SD		2.6584	0.2359	1.3688	1.38		2.6876	0.2411	1.381	1.40

Figure 3.7 Calculated radiogenic heat production values using Rybach (1988) and compared to those calculated by Reay (2011).

The calculation assumes that radiogenic isotope concentrations are uniform throughout the rock and that a bulk density is used. The density used here (2.594 g cm^{-3}) is for the 'G2' granite facies from one data point in the eastern magmatic centre (Antriasian 2010). The calculation assumes that this is representative of the bulk density of the granite for the Mourne Granite Complex.

3.3.3. Extrapolated Temperature

The extrapolated temperature calculation (Equation 21) for the Silent Valley borehole makes use of the geothermal gradient and bottom-hole temperature.

For 2500 m:

$$T_{ze} = 21.86 + \left[\frac{2500 - 591}{1000} \times \frac{11.608}{0.551}\right]$$

$$T_{ze} = 62.08\ ℃$$

For 5000 m:

$$T_{ze} = 21.86 + \left[\frac{5000 - 591}{1000} \times \frac{11.608}{0.551}\right]$$

$$T_{ze} = 114.76\ ℃$$

The calculation assumes a constant geothermal gradient which has been calculated over a short depth range.

4. Interpretations

The three profiles have been examined and interpreted with three dimensions in mind. Details of these interpretations are described below with a particular focus on the geothermal targets than can be inferred in each section.

4.1. Geological and geothermal interpretations from 2D modelling

The models are discussed individually below. The simple geological setting of a relatively homogenous country rock of conductive siltstones relative to the resistive intrusive granite means that attributing rocks to specific resistive or conductive zones is quite straight forward. Resistive features are represented by purple-blue colours whereas conductive features are green-yellow-red.

4.1.1. Interpreted 2D EMC model

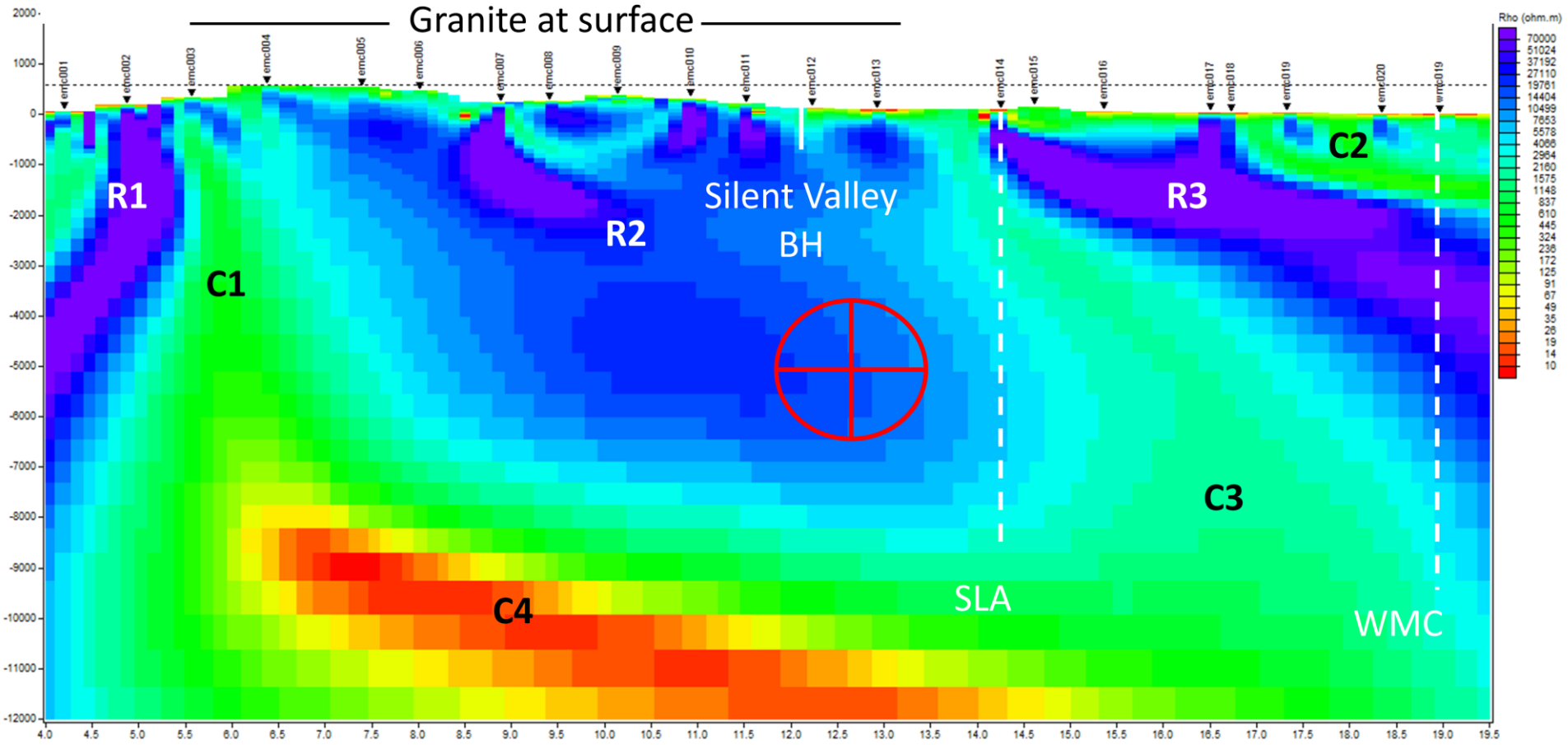

Figure 4.1 2D model of profile EMC with interpretation and reference to other profiles and the Silent Valley borehole.

The EMC profile model (Fig.4.1.) shows a near vertical resistor (R1) at the northern most extent of the profile, interpreted as granite. The vertical nature of this granite body is reminiscent of a steep wall contact, commonly associated with cauldron subsidence models. The close proximity of a similarly vertical conductor (C1), however, complicates interpreting this as a wall feature (which would require a vertical slab of country rock to be trapped on the inside of the 'cauldron'). It is difficult to account for such a geometry in geological terms, however, it does not appear critical when assessing the geothermal energy potential of the area.

The model is dominated by a large central resistor (R2) and has a similar cross-sectional length as the granite at the surface. It is interpreted that R2 relates to the bulk of the eastern magmatic centre and extends to a depth of 7 km. It may be possible through further petrological and petrophysical analysis to distinguish between different granite facies in this block as part of a layered intrusion: the more mafic 'G1' facies which tops Slieve Donard (near emc004, emc005 and emc006) may have a lower resistivity compared to that of 'G3' (10,000-30,000 Ω.m; Kelly 2010) which is found in the Silent Valley borehole. The flat-lying resistor (R3) is similar to that of a laccolithic granite intrusion. The thickness of this granite body (~2 km) is in keeping with quoted laccolith thicknesses (Aranguren *et al*. 2003; Westerman *et al*. 2004). The overlying conductor (C2) is interpreted as the Silurian country rock; the weak conductive layer at the top of the profile in the mountain areas relates to weathered granite. Conductor C3 has been labelled as it may be a zone of country rock underlying the laccolith. The higher resistivity associated with C3 may be partly a result of the smoothing inherent in the 2D inversion modelling or it may be a real geological effect such a thermal metamorphism relating to the intrusion of the granite. The conductor underlying the mountains (C4) is unexpected. C4 may relate to a ductile shear zone, brine-rich rock or even a sulphide or graphite mineral deposit. Interpretations for the origin of C4 are tentative and, as C4 is below the target depth for geothermal exploration, it will not be discussed further.

The crosshair at the base of R2 highlights a potential geothermal target in terms of a favourable depth extent, falling in the depth range of 4-5 km.

Model testing for the EMC profile indicates that the depth of R2 is quite well constrained in that it cannot be thinned without affecting the RMS error. In terms of extending the thickness to greater depths, this is less well constrained and appears that granite may exist deeper to 18km before RMS errors increase by >10%. The potential

for the granite to extend to this depth calls into question the existence of C4 which has been tested and appears that apparent resistivities can be >3500 Ω.m and still provide reasonable RMS error values. The connectivity of R1 and R2 was also tested and it appears that the MT data require the presence of C1. However, connectivity between R2 and R3 in the south may well be possible at shallow depths (upper 1-2 km) without significantly increasing the RMS error. The connectivity between R2 and R3 would support laccolithic emplacement, however, the need for a steep boundary between R1 and R2 would infer a wall-like contact as seen in the cauldron subsidence model. It may be that a hybrid of the two emplacement mechanisms is plausible, with a piston-like steep fault in the north being 'jacked up' by laccolithic emplacement from the south.

4.1.2. Interpreted 2D WMC model

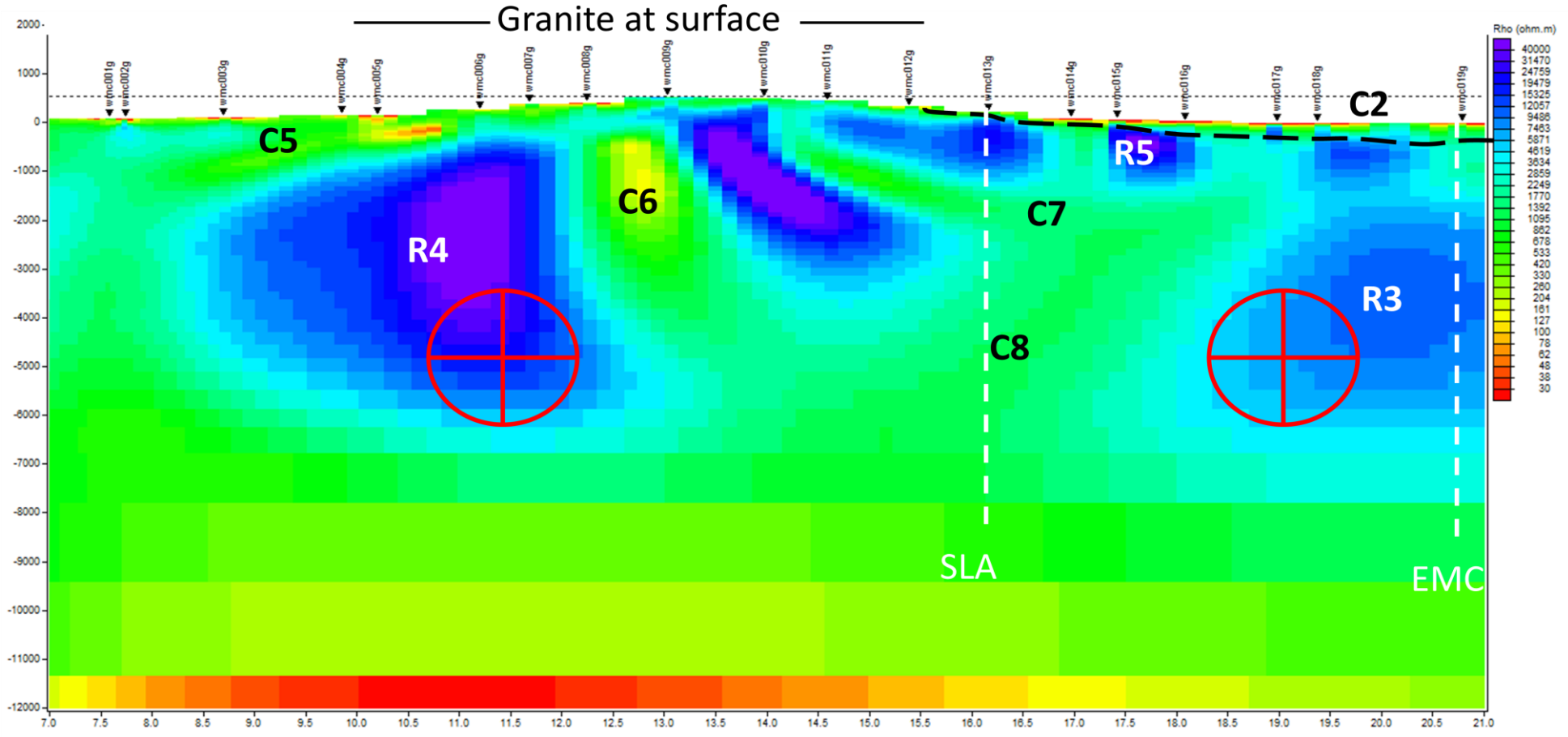

Figure 4.2 2D model for profile WMC with interpretations and reference to other profiles.

The model for profile WMC (Fig.4.2.) is somewhat different to that of EMC. There is no northern vertical resistor (e.g. R1) and the profile actually extends further north off of the western magmatic centre toward the Newry Granodiorite. The most northern resistor (R4) underlies much of the northern flank of the western magmatic centre and it is interpreted that R4 is granite relating to that body. It appears to have a shallow contact with conductor C5 but granite should actually be present at the surface according to current geological maps (Fig.). C5 may be a feature of the Newry fault which runs nearby to site wmc005 and the most conductive parts of the conductor may be associated with the fault system.

Conductor C6 separates a R4 into two portions. C6 is interpreted to be a fault zone as testing revealed that the model can accommodate this as a more resistive feature without detrimental effects on the RMS error.

R5 represents a tabular granite which is interpreted as a laccolithic structure. The changes in modelled resistivity along R5 can be accounted for by static shifts in the data causing a low apparent resistivity value at some sites. R5 is overlain by C2 which is again Silurian country rock. R5 appears to be connected to the resistor R3 and R3 could be inferred as a source of magma. R5 could therefore be a branch of granite from a magma chamber flowing from south to north. R3 has been labelled the same as in the EMC model as it is interpreted as being a cross-section through the low-angle resistor in the south of the EMC profile. R3 may therefore correspond with a conduit of granite magma flow which relates to both the eastern and western magmatic centres.

C7 is interpreted as a slab of country rock underlying R5 and the same can be said for C8.

The general shape of the western magmatic body is difficult to interpret and appears to be related to a lopolithic mechanism (doming downwards into the country rock) rather than inflating upwards as in laccolith emplacement. The granite geometry is complicated by the interpreted fault zone, C6, and the presence of C7. Model testing to see if conductors C7 and C8 are required revealed that forcing the model to be resistive at C7 and C8 actually improved the RMS error. However, this modification results in a model that has a thin ‘rim’ of conductive matter surrounding a large resistive block and is not representative of a reasonable geological scenario and can be rejected. The fact the MT data requires a thin conductor in the model, even when forced to be resistive indicates that C7 and C8 are necessary and quite robust features of the model.

Model testing of the depth extent of the granites showed that it is difficult to reduce the thickness of the granite across the model by >1 km. The thickness, however, can be increased by >3 km. The maximum depth and thickness of the granites is poorly constrained due the limited depths of penetration achieved because of weak signal during data recording. Essentially the base of the granites in the western magmatic centre appears comparatively shallow compared to that of the eastern magmatic centre.

Potential geothermal targets have been identified in the WMC model and are marked by crosshairs. R4 is purely identified in terms of favourable depth extent whereas R3 has also now been highlighted (it is omitted as a target on the EMC profile) as the shape of the body is better constrained, appearing quite tubular.

It should be noted that the EMC model shows quite good connectivity between resistors in the south; testing revealed the importance of steep boundaries in the north of the model and the places where resistors may well be connected. Good connectivity between resistors is likely due to flow direction from the SSW inferred by Stevenson *et al*. (2007) for the eastern magmatic centre being approximately along the EMC profile. The flow direction for the western magmatic centre inferred by Stevenson & Bennett (2011) is again from the SSW, however, the profile cuts obliquely to the flow direction. Therefore, in the WMC model, features such as country rock (particularly C7) may not represent a complete block to magma flow and may be rafts trapped within the granite, where granite has flowed around on either side in areas outside of the 2D modelled section.

4.1.3. Interpreted 2D SLA model

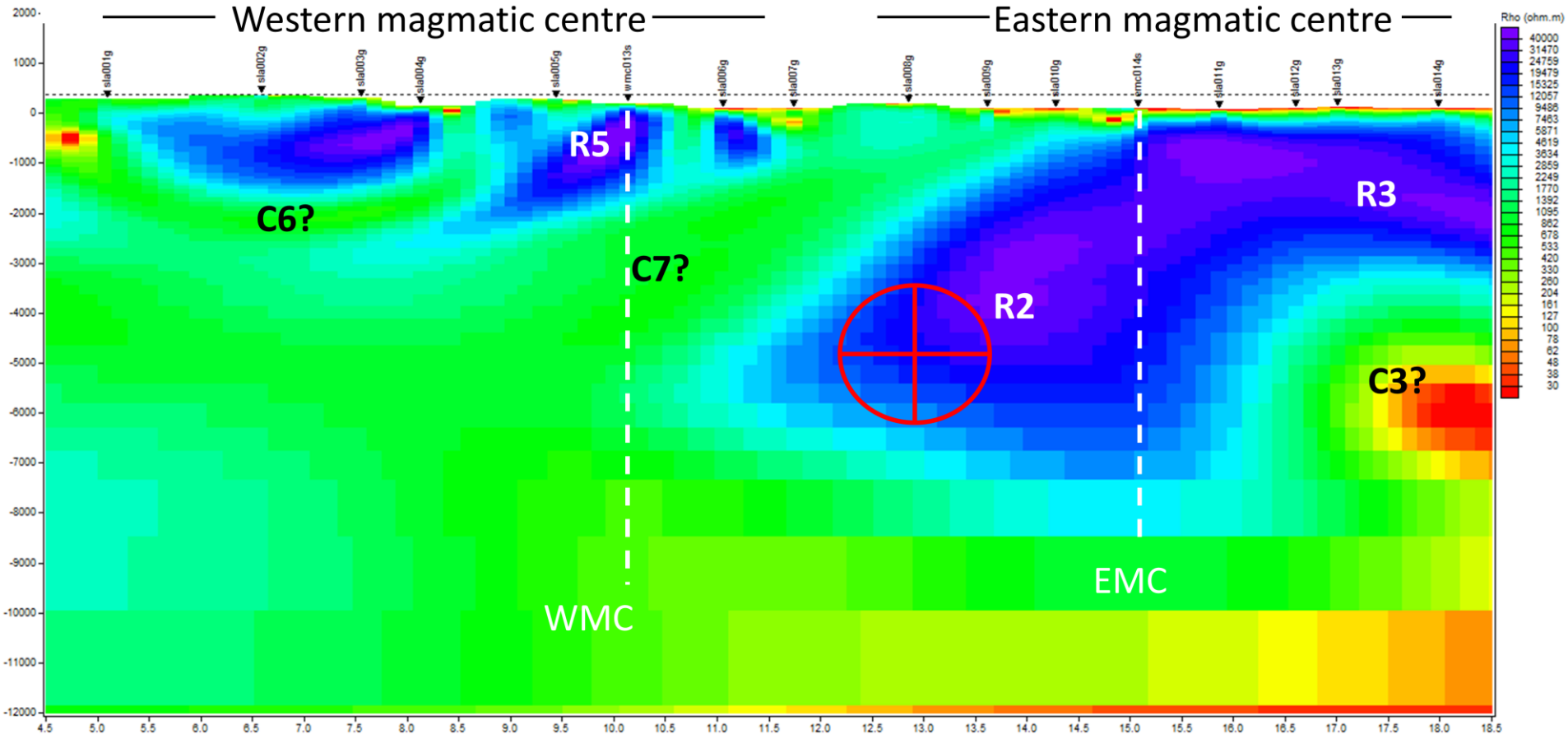

Figure 4.3 2D model for profile SLA with interpretations and reference to other profiles.

The SLA profile model (Fig.4.3.) presents no new features but provides an excellent model from which the 3D structure can begin to be inferred from 2D modelling. R5, associated with the western magmatic centre, can be interpreted more definitely as a sheet-like tabular granite. The thickness can be quite well constrained to approximately 2 km (model testing reveals this is a minimum thickness) and the east-west extent of the sheet is ~6 km. C6 has been tentatively inferred and may well be a slab of country rock which does not fully underlie R5 and thus may not be a complete barrier to magma flow as might be inferred from in the WMC model.

R2 and R3 have been interpreted as the same resistor. It has been inferred in this way because of the close proximity to both resistors where the SLA model cuts the EMC model. The 'R3' labelled in the SLA profile is not the direct equivalent of R3 in the EMC profile but likely to be laterally part of the same resistor.

C3 has been inferred in the SLA model, although, this is highly conductive in comparison to that of the EMC model. However, model testing has revealed that this feature may be another fault zone as C3 in the SLA model can equally be accommodated as a more resistive zone, potentially as resistive as R3. It may be that this potential fault zone existed before granite emplacement and may have acted as a pathway that magma exploited. C3 in the SLA model is difficult to constrain as it is on the edge of the model, extending the profile would help aid constraints on this area.

C7 has been tentatively interpreted as a slab of country rock trapped between the two magmatic centres. Model testing shows that this is a robust feature and an important part of the SLA model. Geologically, this potential slab of country rock is of great interest and adds significant weight to the laccolithic emplacement argument. The earlier eastern magmatic centre in a cauldron subsidence model would be undercut by the later western magmatic centre. Sheet-like intrusion and inflation in line with that of a laccolith emplacement model can explain the presence of country rock separating the two centres and also explain why the younger western magmatic centre does not cut the eastern centre. Two sheets may not necessarily intrude at the same level (in this case the western magmatic centre appears shallower) and if the sheets subsequently were to inflate (not necessarily contemporaneously) a diagonal block of country rock would be trapped. In some cases this inflation can lead to the two sheets meeting and wholly consuming the country rock to create a large xenolith.

Granite thickness has been tested and found that the thicknesses observed in the model for each magmatic centre are a minimum thickness; reducing granite thickness resulted in a significant jump in the RMS error. The total depth extent, however, is poorly constrained due to poorer penetration depth relating to weak signal during the recording period.

A potential geothermal target for R2 has been identified again in the SLA model. The model provides a better understanding of the shape of the granite body, which may well be laterally connected to R3 and which could not be determined unequivocally in the EMC model alone.

4.2. Inference of geothermal calculations

The geothermal calculations show some important characteristics of the Mourne Granite Complex as a potential geothermal target.

Heat flow modelling by Goodman *et al*. (2006) shows good agreement with the calculated heat flow of 73.31 mW m^{-2} for the Silent Valley borehole. The calculated heat flow value for this report would indicate that those values calculated by Brock (1989) are in fact somewhat overestimated (84 and 87 mW m^{-2}). Despite a lower calculated heat flow value than Brock (1989), it is still elevated compared to the average UK value of 55 mW m^{-2} quoted by Rollin (1987). Importantly, the calculated heat flow value presented here is for the Mourne granite, specifically the 'G3' granite facies. Heat flow also needs to be considered for the Silurian siltstones and mudstones. Data do not currently exist, however, a low heat flow value relative to that calculated for the granite and an associated low thermal conductivity would provide good insulation to the granite and help contain heat within the granite.

The average heat production for all samples calculated using Rybach (1988) has a high value of 6.44 µW m^{-3} ± 1.38 and can be considered quite reliable, being determined from direct XRF data rather than the aerial radiometric measurements of the TELLUS survey. Interestingly, the heat production values calculated for separate granite facies vary quite considerably and may well relate directly to the magma evolution described in Meighan *et al*. (1988) and McCormick *et al*. (1993). The individual values calculated here, using Rybach's (1988) equation, compare well with the results from the heat production equation used by Reay (2011) the same as the equation used by van Dam (2007). The average heat production for all samples calculated using the XRF data is

significantly higher than the uppermost value calculated by van Dam (2007). Van Dam's work made use of the aerial TELLUS data where the amplitude of the effective radioelement concentration measurements can be attenuated by the air, thus giving a lower maximum value of 4.8 µW m^{-3}. Work by van Dam, however, is still important as it shows the spatial distribution and variation of heat production in the Mourne Granite Complex which can be approximately attributed to each granite facies (see Fig.4.4.). Although values for 'G3' are absent, a relatively good agreement exists between the eastern magmatic centre; 'G1' especially shows good agreement with low spatial heat production of van Dam (2007) and the calculated heat production of 3.69 µW m^{-3}. The western magmatic centre has much better calculated heat production values than may be inferred from the spatial distribution according to van Dam (2007). These lows seen in van Dam (2007) are likely to be a misrepresentation in the original aerial radiometric data which can be explained by the land-use at the surface. The area of land represented by 'G5' is partially forested which approximately corresponds to the strong low in the bottom-centre of the surface outcrop. Thus, heat production is good in both the magmatic centres.

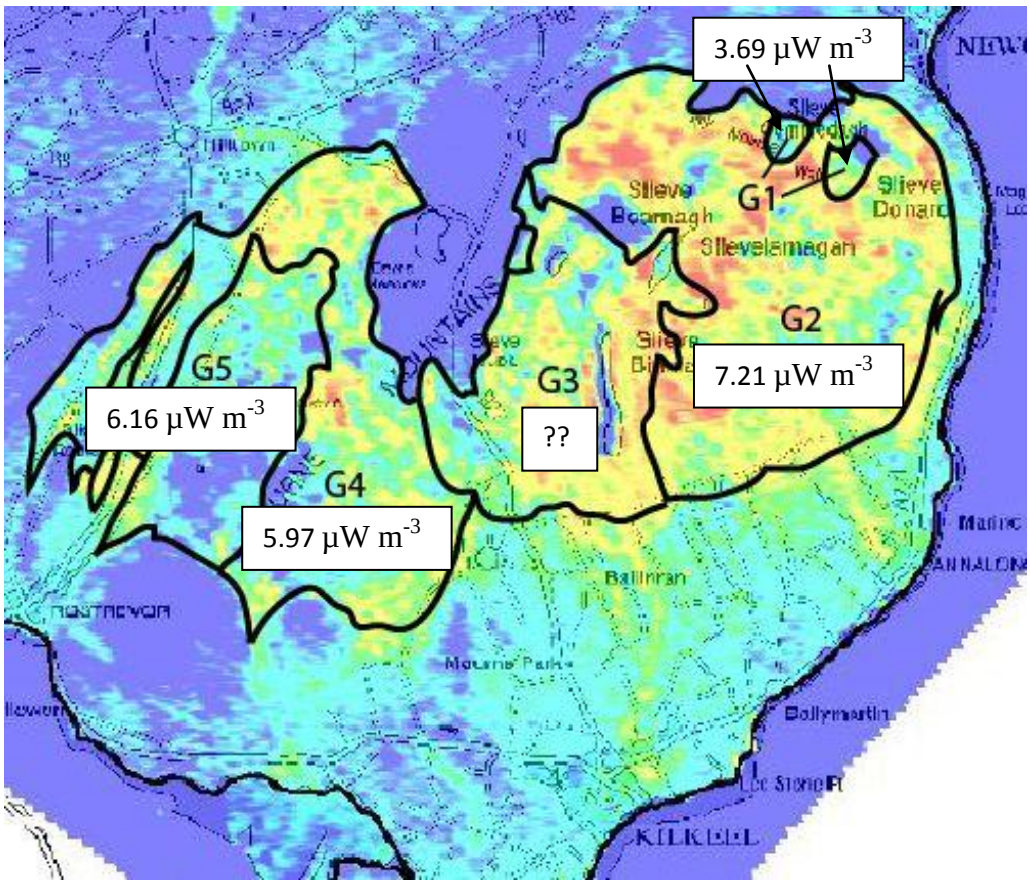

Figure 4.4 Spatial representation of heat flow from van Dam (2007) with granite facies and the calculated heat production from this study annotated for each facies.

The extrapolated temperature to a depth of 2500 m (62.08 °C) shows reasonable agreement with the modelled temperature at 2500 m by Goodman *et al*. (2004) (approximately 60 °C) with our calculation from the Silent Valley borehole perhaps suggesting a slightly higher value than that modelled. The extrapolated temperature to a depth of 5000 m (114.76 °C) is perhaps more important when considering a geothermal resource for EGS and the calculated value of 114.76 °C. It is important to keep in mind that the calculation assumes a constant geothermal gradient and does not take into account potential variations in radiogenic heat flow, heat production or thermal conductivity with depth. The calculated value of 114.76 °C is an encouraging indicator for actual temperature at this depth as this value is a on the fringe of target temperatures for electricity generation. Temperatures of fluids used in current geothermal projects across the globe are listed below (Fig.4.5; from Bertani 2005):

Country	Water Temp (°C)	Power output (MW)	Energy output (GWh)
Australia	98	0.2	0.5
Austria	105	1.2	3.2
China	140-160	28	96
Germany	98	0.2	1.5
Thailand	116	0.3	1.8
Alaska, USA	74	0.4	n/a

Figure 4.5 Global low-enthalpy geothermal power generation. In comparison, high-enthalpy sources from 16 different countries produce a combined 9000 MW of electrical power.

5. Conclusions

2D inversion modelling of the three MT profiles has yielded some interesting results with respect to determining the subsurface distribution of the granite in terms of shape, depth extent and volume. These are summarised below:

i. The emplacement mechanism is the overriding control on the subsurface distribution of the granite. 2D MT modelling has shown that the emplacement mechanism probably does not adhere to a simple end-member model and has not proven a cauldron subsidence model or a laccolithic emplacement model. While the modelling has not been completely conclusive, features of both styles of emplacement have been identified and it could be inferred that a hybrid of the two emplacement mechanisms has occurred.

ii. While resistors R3 and R5 are better constrained in terms of shape, the overall shape of both magmatic centres, centrally and for the potential feeder zones along the flanks, is still difficult to constrain with high certainty.

iii. The depth extent for the two magmatic centres has been particularly interesting and shows that while a relatively constant depth can be seen at the base of the eastern magmatic centre, the western magmatic centre appears to get deeper further north. Furthermore, the inference of laccolithic bodies in the SLA model shows a significant change in thickness, with the younger, western laccolith being much thinner than the eastern. Whilst minimum thickness have generally been well constrained from model testing throughout each of the models and is probably the most useful feature to be constrained when assessing the geothermal energy potential. The constraints on the maximum possible thickness has been quite variable. Poor constraints on the maximum possible thickness relates to poor signal quality during recording and limited depth of penetration, particularly in the SLA and the WMC models. The potential to extend the resistors to greater depths in the EMC model however, is unusual. While acceptable RMS errors are achievable when forcing the model resistors be resistive to greater depths, when left ‘unlocked’ the resistors in the model do revert back to being similar to their configuration in the final model. Thus, it is taken that the final model provides the best fit to the observed data and that greater depths, although feasible in modelling terms, are probably less plausible.

iv. Identifying the volume from 2D models was deemed inappropriate. While the apparent cross-section through R3 in the EMC and WMC models and to some

extent in the SLA model, it would be an assumption that these are representative of a width, length and depth, all orthogonal to each other and are unlikely to provide an accurate volume. Furthermore, additional sections through the main magmatic centres would also be required to identify their volume.

v. The identification of three potential geothermal targets has been based on the favourable depth extent of resistors R2 and R4, but also with a tentative interpretation of the shape of the granite intrusion with respect to R3 on profile WMC.

The heat flow, heat production and extrapolated temperature calculations all reveal encouraging values for development of the Mourne Granite Complex as a geothermal resource. While the temperatures are on the fringe of target values for electricity generation, they may well be adequate for significant space heating. Calculations herein are proposed as reasonable estimates on temperature with depth as an average temperature gradient is used, the assumption of minimal changes in heat production and thermal conductivity would suggest the geothermal gradient may well be steady. Granites underneath Silurian country rock to the south may be hotter due to insulation from the overlying sediments.

To overcome problems outlined with regard to the subsurface distribution of the granite, it is recommended further work be undertaken to increase the number of MT sites for both the EMC and SLA profiles. More sites will provide a fresh data source which may have better signal to constrain the maximum depth of the granites in the area. It may be that the data adequately samples the target region of <10 km depth due to the "MT foot print" where the depth of penetration approximately equates to the lateral extend of data sampling away from the site (e.g. 5 km penetration depth will have approximately a 5 km diameter of data sapling at 5 km depth), additional data, however, could be used to replace site with bad data (e.g. emc001 and emc002). Extension of these profiles will also allow for the ends of the models to be better constrained (e.g. R1 and C4). Further profiles, three or more, should also be taken through the centre of the magmatic centres to help determine the volume of the main bodies. More profiles will allow for a grid of MT sites and make 3D inversion modelling feasible, which may provide a better grasp of the shape, depth extent and volume of the granites and perhaps lead to a more certain identification of the emplacement mechanism for the Mourne Granite Complex.

Further geophysical modelling could be undertaken, particularly for 2D or even 3D gravity modelling, which would provide valuable estimates on the volume of the granites, particularly if constrained by the existing MT models presented here.

It is critical that further work measures the thermal conductivity of the Silurian sediments, particularly in the south of the Mourne area, to ascertain their potential as a thermal blanket to the underlying granite inferred in the MT models presented here.

When assessing the area in advance of a drilling program, the stress fields in the granite would need to be measured and accounted for whilst drilling and 'fracking' to create the fracture network required for development of an EGS target.

Acknowledgements I would like to thank Laura Ayres (University of Birmingham) for her collaboration throughout the project, Dr Carl Stevenson (University of Birmingham) and Dr Mark Muller (DIAS) for supervision during the project, Derek Reay (GSNI) for various resources and funding, Orla Gallagher (GSNI, now at Dalradian Gold Ltd) and Claire McGinn (GSNI) for site permitting prior to the geophysical survey as well as the Mourne Heritage Trust (John McAvoy and Dave Farnan), the Mourne Trustees, Forestry Service, Northern Ireland Water, the National Trust and all local farmers for use of their land. I would also like to thank Colin Hogg (DIAS), Mohammed Desissa Ture (GSNI), Maryam Hussein (DIAS, now at University of Edinburgh), Ciaran Chittock, Siobhan Austin (both Methodist College, Belfast) and Tom Henderson (University of Plymouth).

6. References

Antriasian, A. 2010. Thermal conductivity, density, specific heat, diffusivity, porosity and permeability analysis of core specimens. Hot Dry Rocks Pty Ltd. *Report for the Geological Survey of Northern Ireland*.

Aranguren, A., Cuevas, J., Tubía, RomÁn-Berdiel, T., Casas-Sainz, A. & Casas-Ponsati, A. 2003. *Journal of the Geological Society*, **160**: 435-445.

Anderson, T.B. 2004. Southern Uplands-Down-Longford Terrane. *In* The Geology of Northern Ireland – Our Natural Foundation. Mitchell, W.I. *(ed.)*. Second Edition. Geological Survey of Northern Ireland, Belfast.

Anderson, T.B., Johnston, T.P. & Mitchell, W.I. 2004. Basement Structure and the Terrane Model. *In* The Geology of Northern Ireland – Our Natural Foundation. Mitchell, W.I. *(ed.)*. Second Edition. Geological Survey of Northern Ireland, Belfast.

Ayres, L., Yeomans, C., Stevenson, C., Muller, M., Reay, D. & Desissa Ture, M. 2011. Constraints from magnetotellurics on the subsurface structure and emplacement of the Mourne Granites. *54th Irish Geological Research Meeting*, Galway. NUIG, 18th-20th February 2011.

Bertani, R., 2005. World geothermal power generation in the period 2001 – 2005. *Geothermics*, **34**: 651–690.

Bostick, F.X. & Smith, H.W. 1962. Investigation of Large-Scale Inhomogeneities in the Earth by the Magnetotelluric Method. *Proceedings of the IRE (IEEE)*, **50**: 2339-2346. *Reprinted In*, Magnetotelluric Methods, Vozoff, K. *(ed.)*. Society of Exploration Geophysicists, Geophysics reprint series No.5, 1986. Pages 148-155.

Brock. A. 1989. Heat flow measurements in Ireland. *Tectonophysics*, **164**: 231-236.

Brock, A. & Barton, K. 1984. Equilibrium temperature and heat flow density measurements in Ireland. Commission of the European Communities, Brussels, EUR 9517.

Cagniard, L. 1953. Basic theory of the magneto-telluric method of geophysical prospecting. *Geophysics*, **18**: 605-635. *Reprinted In*, Magnetotelluric Methods, Vozoff, K. *(ed.)*. Society of Exploration Geophysicists, Geophysics reprint series No.5, 1986. Pages 4-34.

Carmichael, R.S. 1989. Practical Handbook of Physical Properties of Rocks and Minerals. CRC Press, Inc. ISBN 0-8493-3703-8.

Čermák, V. & Rybach, L. 1979. Terrestrial Heat Flow in Europe. Springer. Berlin.

Cook, A.H. & Murphy, T. 1952. Gravity Survey of Ireland north of the line Sligo-Dundalk. *In* Measurements of Gravity in Ireland. *Geophysical Memoir, Dublin Institute for Advanced Studies*, **2**: 17-20.

North of the line Sligo-Dundalk. *In*. Measurements of Gravity in Ireland. *Dublin Institute for Advanced Studies, Geophysical Memoir No. 2*, **Part 4**: 17-20.

Cooper, M.R. 2004: Palaeogene Extrusive Igneous Rocks. *In* The Geology of Northern Ireland – Our Natural Foundation. Mitchell, W.I. *(ed.)*. Second Edition. Geological Survey of Northern Ireland, Belfast.

Cooper, M.R., & Johnston, T.P. 2004. Palaeogene Intrusive Igneous Rocks. *In* The Geology of Northern Ireland – Our Natural Foundation. Mitchell, W.I. *(ed.)*. Second Edition. Geological Survey of Northern Ireland, Belfast.

Desissa Ture, M. 2011. *Personal Communication*. Geological Survey of Northern Ireland, Belfast.

Garcia, X. & Jones, A.G. 2002. Atmospheric sources for audio-magnetotelluric (AMT) sounding. *Geophysics*, **67**: 448-458.

Gamble, T.D., Goubau, W.M. & Clarke, J. 1979. Magnetotellurics with a remote magnetic reference. *Geophysics*, **44**: 53-68.

Gamble, J.A., Wyscozanski, R.J. & Meighan, I.G. 1999. Constraints on the age of the British Tertiary Volcanic Province from ion microprobe U–Pb (SHRIMP) ages for acid igneous rocks from NE Ireland. *Journal of the Geological Society, London*, **156**: 291-299.

Geothermal Engineering Ltd, 2011. http://geothermalengineering.co.uk/page/geothermal-background.html. **Accessed 07/04/2011**.

Gibson, D. 1984. The petrology and geochemistry of the western Mournes granites, Co. Down. Unpublished Ph.D thesis, Queen's University Belfast.

Gibson, D., McCormick, A.G., Meighan, I. G. & Halliday, A.N. 1988. The British Tertiary Igneous Province; Young Rb-Sr ages for the Mourne Mountains Granites. *Scottish Journal of Geology*, **23**: 221-225.

Goodman, R., Jones, G.L.I, Kelly, J., Slowey, E. & O'Neill, N. 2004. Geothermal Energy Resource Map of Ireland. CSA Group *for* Sustainable Energy Ireland.

Groom, R.W. & Bailey, R.C. 1989. Decomposition of Magnetotelluric Impedance Tensors in the Presence of Local Three-Dimensional Galvanic Distortion. *Journal of Geophysical Research*, **94**: 1913-1925.

Gupta, M.L., Sundar, A. & Sharma, S.R. 1991. Heat flow and heat generation in the Archaean Dharwar cratons and implications for the Southern India Shield geotherm and lithospheric thickness. *Tectonophysics*, **194**: 107-122.

Harinarayama, T., Abdul Azeez, K.K., Murthy, D.N., Veeraswamy, K., Eknath Rao, S.P., Manoj, C. & Naganjaneyulu, K. 2006. Exploration of geothermal structure in Puga geothermal field, Ladakh Himalayas, India by magnetotelluric studies. *Journal of Applied Geophysics*, **58**: 280-295.

Hogg, C. 2010. *Personal Communication*. Dublin Institute for Advanced Studies, Ireland.

Hood, D.N. 1981. Geochemical, petrological and structural studies on the Tertiary granites and associated rocks of the Eastern Mourne Mountains, Co. Down, Northern Ireland. Ph.D thesis, Queen's University Belfast.

Jones, A.G. 2011. *Personal Communication*. Dublin Institute for Advanced Studies, Ireland.

Jones, A.G., Chave, A.D., Egbert, G. & Bahr, K. 1989. A Comparison of Techniques for Magnetotelluric Response Function Estimation. *Journal of Geophysical Research*, **94**: 14,201-14,213.

Jones, A.G. & Groom, R.W. 1993. Strike-angle determination from the magnetotelluric impedance tensor in the presence of noise and local distortion: rotate at your peril! *Geophysical Journal International*, **113**: 524-534.

Kelly, J. 2010. Deep Geothermal Exploration Drilling AES Kilroot Power Station and Silent Valley Reservoir Area. SLR. *Report for the Geological Society of Northern Ireland*.

Lapworth, C. 1878. The Moffat Series. *Quarterly Journal of the Geological Society of London*, **34**: 240-346.

Madden, T. And Nelson, P. 1986. A defence of Cagniard's magnetotelluric method. *Unpublished Report*, Geophysics Lab, Office of Naval Research, MIT, Cambridge Massachusetts. Magnetotelluric Methods, Vozoff, K. *(ed.)*. Society of Exploration Geophysicists, Geophysics reprint series No.5, 1986. Pages 89-95.

Martí, A. 2006. A Magnetotelluric Investigation of Geoelectrical Dimensionality and Study of the Central Betic Crustal Structure. Dissertation, Department de Geodinmica i Geofsica, Universitat de Barcelona.

McNiece, G.W. & Jones, A.G. 2001. Multisite, multifrequency tensor decomposition of magnetotelluric data. *Geophysics*, **66**: 158-173.

Meighan, I.G., Gibson, D. & Hood, D.N. 1984. Some aspects of Tertiary acid magmatism in NE Ireland. *Mineralogical Magazine*, **48**: 351-363.

Meighan, I.G., Fallick, A.E. &McCormick, A.G. 1992. Anorogenic granite magma genesis: new isotopic data from the southern sector of the British Tertiary Volcanic Province. *Transactions of the Royal Society of Edinburgh: Earth Sciences*, **83**: 227-233.

Merriman, R.J. & Roberts, B. 2001 (for 2000). Low grade metamorphism in the Scottish Southern Uplands terrane: deciphering the patterns of accretionary burial, shearing and cryptic aureoles. *Transactions of the Royal Society of Edinburgh: Earth Sciences*, **91**: 521-537.

Miensopust, M. P. 2010. Multidimensional magnetotellurics: a 2D case study and a 3D approach to simultaneously invert for resistivity structure and distortion parameters. Ph.D thesis, Dublin Institute for Advanced Studies & National University Ireland Galway.

Monnet, B.J. 1981. Investigation of the geothermal potential of the UK: a preliminary assessment. Institute of Geological Sciences. *Commission of the European Communities*.

Palacky, G.J. 1987. Resistivity characteristics of geological targets. *In*. Electromagnetic Methods in Applied Geophysics, Nabighian, M.N. *(ed)*. Vol. 1 – Theory, Chapter 3: 53-129. Society of Exploration Geophysicists, Tulsa, OK.

Reay, D. 2004. Geophysics and Concealed Geology. *In* The Geology of Northern Ireland – Our Natural Foundation. Mitchell, W.I. *(ed.)*. Second Edition. Geological Survey of Northern Ireland, Belfast.

Reay, D. 2011. Unpublished data, GSNI, Belfast.

Richey, J.E. 1927. Structural relations of the Mourne Granites (Northern Ireland). *Quarterly Journal of the Geological Society of London,* **83**: 653-688.

Rodi, W. & Mackie, R.L. 2001. Nonlinear conjugate gradients algorithm for 2-D magnetotelluric inversion. *Geophysics,* **66**: 174-187.

Rohleder, H.P.T. 1932. A tectonic analysis of the Mourne granite mass, County Down. *Proceedings of the Royal Irish Academy,* **41**: 160-174.

Rollin, K.E. 1987. Catalogue of geothermal data for the land area of the United Kingdom. British Geological Survey, 3rd Review.

Rybach, L. 1976. Radioactive heat production in rocks and its relation to other petrophysical parameters. *Pure and Applied Geophysics*, **144**: 309-318.

Rybach, L. 1988. Determination of heat production rate. *In*, Handbook of Terrestrial Heat-Flow Determination, Hänel, R., Rybach. L. and Stegena, L. *(eds)*. Kluwer Academic Publishers, Dordrecht, pp. 125–142

Sims, W.E., Bostick, F.X. Jr & Smith, H.W. 1971. The estimation of magnetotelluric impedance tensor elements from measured data. *Geophysics*, **36**: 938 – 942.

Simpson, F. & Bahr, K. 2005. Practical Magnetotellurics. Cambridge University Press.

Stevenson , C.T., Owens, W.H., Hutton, D.H.W., Hood, D.N. & Meighan, I.G. 2007. Laccolithic, as opposed to cauldron subsidence, emplacement of the Eastern Mourne pluton, N. Ireland: evidence from anisotropy of magnetic susceptibility. *Journal of the Geological Society of London,* **164**: 99-110.

Stevenson, C. T. 2011. *Personal Communication*. University of Birmingham, UK.

Stevenson, C.T. E. & Bennett, N. 2011. The emplacement of the Palaeogene Mourne Granite Centres, Northern Ireland: new results from the Western Mourne Centre. *Journal of the Geological Society of London*, **168**: 1-6. doi: 10.1144/0016-76492010-123.

Swift, C.M. 1967. A magnetotelluric investigation of an electrical conductivity anomaly in the southwestern United States. Ph.D thesis, MIT, Cambridge, MA. *Extract Reprinted In*, Magnetotelluric Methods, Vozoff, K. *(ed.)*. Society of Exploration Geophysicists, Geophysics reprint series No.5, 1986. Pages 156-166.

Tikhonov, A.N. 1950. On determining electrical characteristics of the deep layers of the Earth's crust. *Doklady*, **73**: 295-297. *Reprinted In*, Magnetotelluric Methods, Vozoff, K. *(ed.)*. Society of Exploration Geophysicists, Geophysics reprint series No.5, 1986. Pages 2-3.

Uchida, T. 2009. Magnetotelluric investigation for geothermal resources. *I-GET Final Conference: Geophysics and Geology in Geothermal Exploration*. 23/24 February 2009, Potsdam, Germany.

Van Dam, C.L. 2007. Radiogenic thermal heat potential of Northern Ireland. *Report for the Geological Survey of Northern Ireland*.

Walker, G.P.L. 1975. A new concept of the evolution of the British Tertiary intrusive centres. *Journal of the Geological Society, London,* **131**: 121-141.

Wait, J.R. 1954. On the Relation between telluric currents and the Earth's magnetic field. *Geophysics*, **19**: 281-289. *Reprinted In*, Magnetotelluric Methods, Vozoff, K. *(ed.)*. Society of Exploration Geophysicists, Geophysics reprint series No.5, 1986. Pages 35-43.

Westerman, D.S., Dini, A., Innocenti, F. & Rocchi, S. 2004. Rise and fall of a nested Christmas-tree laccolith complex, Elba Island, Italy. *Geological Society of London, Special Publications*, **234**: 195-213.

Wheildon, J., Gebski, J.S. & Thomas-Betts, A. 1985. Further investigation of the UK heat flow field (1981-1984). British Geological Survey Report.

Wright, J.E., Hull, J.H., McQuillin, R. & Arnold, S.E. 1971. *Irish Sea Investigations 1969-70*. Irish Geological Survey Report, **71/19**.